Reliability Assessment of a Continuous-state Fuel Cell Stack System with Multiple Degrading Components

A dissertation presented to

the faculty of

the Russ College of Engineering and Technology of Ohio University

In partial fulfillment

of the requirements for the degree

Doctor of Philosophy

Xinying Wu

August 2019

This dissertation titled

Reliability Assessment of a Continuous-state Fuel Cell Stack System with Multiple Degrading Components

by

XINYING WU

has been approved for

the Department of Industrial and Systems Engineering

and the Russ College of Engineering and Technology by

Tao Yuan

Associate Professor of Industrial and Systems Engineering

Dennis Irwin

Dean, Russ College of Engineering and Technology

ABSTRACT

XINYING WU, Ph.D., August 2019, Mechanical and Systems Engineering

Reliability Assessment of a Continuous-state Fuel Cell Stack System with Multiple Degrading Components

Director of Dissertation: Tao Yuan

This study is motivated by a degradation experiment conducted by an industrial collaborator on the long-term durability of a polymer electrolyte membrane fuel cell (PEMFC) stack. A PEMFC stack can be considered as a multi-component system composed of continuously degrading fuel cell components. The voltage degradation of the fuel cells causes the degradation of the stack system. The system degradation is assessed by using two system-level degradation measures: the overall stack output voltage and the minimum voltage of individual cells. This dissertation proposes a hierarchical Bayesian approach to predict the failure-time distribution of a stack which is randomly selected from its population and the remaining useful life (RUL) of a monitored PEMFC stack system by using the voltage degradation data collected from its fuel cell components. A two-term exponential function is adopted to describe the mean voltage degradation-paths of the fuel cell components and a hierarchical Bayesian degradation model is established to predict the stack system reliability. A Gibbs sampling algorithm is developed for the inference of the parameters in the hierarchical degradation model. Three alternative modeling approaches are explored and compared.

This research will contribute to the degradation modeling and data analysis methods for continuous-state systems composed of continuous-state components.

DEDICATION

I dedicate this dissertation to my advisor, Dr. Yuan who have supported me throughout the study. I also dedicate this dissertation to my forever love, Ivy who is always the best reason to encourage me moving forward.

ACKNOWLEDGMENTS

During the last five years of my PhD study in Ohio University, lots of persons guided and helped me on my academic research. It would be impossible to complete my study without their encouraging, advising, and supporting.

First, I would like to express my appreciation to my advisor, Dr. Yuan, who suggested the idea for this study, and provided me technical assistance and encouragement during my whole research and academic study. Moreover, he always uses his patience and knowledge to help me overcome any difficult I met.

My additional thanks go to my committee professors: Dr. Diana Schwerha, Dr. Gary Weckman, Dr. Jundong Liu, and Dr. William Young. Thank you for their suggestions, directions, and perceptive comments.

Finally, I would like to appreciate the unconditional support, encourage and love from my family.

TABLE OF CONTENTS

Page

LIST OF TABLES

Page

LIST OF FIGURES

Page

CHAPTER 1: INTRODUCTION

1.1 Objective and Motivation

The objective of this dissertation is to develop a methodology to predict the reliability of continuous-state systems composed of continuous-state components. Traditional system reliability models have been largely based on binary-state or multi-state assumptions which assume a system has a finite discrete set of possible states. The binary-state system reliability modeling and analysis have been used broadly and the binary-state models assume that a system and its components have two states: working or failed [1, 2]. Under the multi-state assumption, a system and its components may exhibit more than two states, such as partially working or partially failed. However, these discrete states assumptions may not be reasonable for some modern systems. For example, A PEMFC stack consists of multiple polymer electrolyte membrane fuel cells [3]. The continuous voltage degradations of the cells cause the performance degradation of the stack system. Therefore, the PEMFC stack system can be considered as a continuous-state system composed of continuous-state components. In recent research, degradation modeling and reliability prediction of a continuous-state system based on degradation testing data of its components have not been fully covered. Thus, a methodology of predicting the reliability of continuous-state systems composed of continuous-state components is highly recommended.

An industrial collaborator conducted a long-term degradation test on a PEMFC stack. Each stack consists of 32 continuously degrading fuel cells. Under a constant power operation condition, voltage behaviors of all fuel cells in one stack were

simultaneously and continuously monitored. All 32 PEMFCs cells are connected in series as show in Figure 1 (see Bae *et al.* [3] for details on the degradation testing procedure and degradation data). This study attempts to propose a hierarchical Bayesian degradation modeling and data analysis method to analyze the system's degradation by using the cells' degradation data. Based on this hierarchical model, the failure-time distribution of a randomly selected stack and the remaining useful life (RUL) of a monitored PEMFC stack can be predicted. Hence, the background of system degradation analysis which is corresponding to this study is introduced first in this chapter.

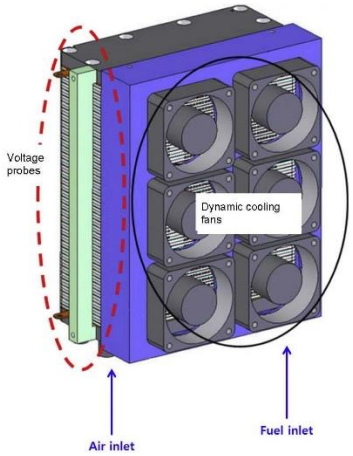

Figure 1. PEMFC system

1.2 Background

This section briefly introduces the backgrounds of reliability, system reliability models, degradation models, and Bayesian methods.

1.2.1 Reliability

Reliability is the probability that a system or a component will perform its function adequately for the intended period of time under the anticipated working

condition [4]. Let a continuous non-negative random variable T denote the failure-time of a unit, the reliability function $R(t)$, for $t \geq 0$, is defined as $R(t) = \Pr(T \geq t)$. Reliability evaluations methods can be categorized as failure-time based methods and degradation-based methods. Traditionally, the reliability of a product is assessed by using the failure-time based methods which need to collect failure-time data from reliability tests or field operations. However, for many modern highly reliable products, it is very difficult to collect enough failure-time data within a reasonable test duration to evaluate the products' reliabilities. Hence, degradation-based modeling and analysis methods that utilize degradation data to predict highly reliable products' reliabilities have attracted increasing attentions in the reliability research and application communities.

In degradation-based reliability models, a product is considered to have failed when its degradation level exceeds a failure threshold (usually this is called a "soft failure"). For example, a critical performance measure of a display device, such as a plasma display panel (PDP) or an organic light-emitting diode (OLED), is its luminosity (i.e., brightness), and a product is considered to have failed when its luminosity falls below 50% of its initial luminosity [5].

Except the above category, the reliability models can also be categorized into binary-state, multi-state, and continuous-state models as mentioned in Section 1.1. The binary-state models correspond to the failure-time based models. Both multi-state and continuous-state models are degradation-based models. The multi-state models assume a product can have a finite discrete set of degrading states; while the continuous-state models assume the state of a product can change continuously overtime.

1.2.2 System Reliability Models

The reliability of a system consisting of multiple components can be evaluated via using either a black-box approach or a white-box approach [6]. The black-box approach considers a system as a single unit and evaluates the system reliability by using failure-time data or degradation data collected at the system level. On the other hand, the white-box approach models and predicts the reliability of a system based on the structure of the system and the reliability data is obtained at the component level.

This study focuses on the degradation modeling and analysis for multi-component systems. The majority of existing studies adopted the black-box approach, which views a system as a single unit, concentrating on the degradation testing and modeling for reliability prediction, and maintenance optimization at the system level. There have been some studies pursuing reliability prediction and maintenance optimization of systems with degrading components using the white-box approach. Those studies usually regarded the system as a binary-state system with continuous-state components. However, there have been very limited studies on continuous-state systems with continuous-state components by using the white-box approach.

The white-box approach possesses the following two advantages over the black-box approach. First, it may be easier to obtain sufficient reliability information and data from the constituting components than from the system. Second, when some complex systems have multiple performance measures, some of the measures are not directly measurable at the system level but are easier to obtain at the component level. For example, the PEMFC stack system has two degradation measures: one is the minimum

cell voltage as a safety measure which can only be monitored at the component level, and the other is the stack output voltage as a performance measure which is based on the degradation data of each cell.

1.2.3 Degradation Models

Under the continuous-state assumption, there are two classes of degradation models: general degradation-path models and stochastic processes. The general degradation-path models essentially are regression-based models, where the independent variable is the time and the dependent variable is the degradation measure. The mean regression functions describe the expected degradation-paths. The general degradation-path models usually use the mean regression functions to define the failure-times or degradation measures. That is, a product is considered to fail when the mean regression function reaches the failure threshold. The noises in the observed degradation data are generally considered as measurement errors. On the other hand, stochastic processes-based models describe the observed degradation data by using a stochastic process such as the Wiener process or the Gamma process, and the noises are an inherent part of the degradation process.

When the degradation model is available, the failure-time distribution of a random product or the RUL of a monitored product can be obtained. A failure-time distribution is a cumulative distribution function which is used to describe the probability of failure by time *t*. A RUL is also a cumulative distribution which is used to present the probability of the remaining lifetime left on a system or a component at a particular time of operation.

Base on the failure-time or RUL predictions, other reliability-related decisions such as the warranty, system design, and maintenance can be made.

1.2.4 Bayesian Methods

Bayesian data analysis is a method of estimating parameters by assigning probabilities to possible parameters values. Let *y* denotes the observed value and $p(y/\boldsymbol{\theta})$ is the conditional probability of *y* conditional on the unknown parameters $\boldsymbol{\theta}$. Bayesian estimation method concludes parameters $\boldsymbol{\theta}$ in terms of probability [7] as following:

$$p(\boldsymbol{\theta}/y) \propto p(\boldsymbol{\theta})p(y/\boldsymbol{\theta}) \tag{1.1}$$

where $p(\boldsymbol{\theta}/y)$ is the posterior distribution and $p(\boldsymbol{\theta})$ is called the prior distribution. In other words, the posterior distribution includes the information from the observed value *y* and the prior. Therefore, Bayesian method could be applied on limited dataset especially when the dataset does not contain sufficient information, prior is a key term to improve the estimation probability.

Speaking of the prior distribution, conjugate prior is a priority choice in the Bayesian analysis due to its practical advantage [8]. A prior is said to be conjugate to the sampling density if the resulting posterior is a member of the same parametric family as the prior [9]. Hence, the computation procedure of deriving posterior has been greatly simplified by assigning conjugate priors especially when the conditional probability includes multiple parameters which will result in more complicated calculations. However, conjugate prior does not always exist in most cases. If any information or data from previous experiments or experts are available, an informative prior could be formulated. If there is no information about the parameters and no conjugate priors exist,

then a non-informative prior can be set which does not affect the model itself to complete the Bayesian model.

In a Bayesian model, the parameter $\boldsymbol{\theta}$ could be a parameters vector which includes multiple parameters. If a population has multiple independent observations of similar objects and each observation has multiple parameters, hierarchical Bayesian model could be applied to estimate parameters with multiple layers. Moreover, unit-to-unit variability among the similar objects can also be modeled by a hierarchical Bayesian model. Gibbs sampler is a Markov chain Monte Carlo (MCMC)-based simulation algorithm to apply in many multidimensional problems [7]. The main idea of Gibbs sampler is that if a Bayesian model includes multiple parameters, $\boldsymbol{\theta} = (\theta_1, \dots, \theta_d)$, each iteration of the Gibbs sampler cycles through the sub-vectors of $\boldsymbol{\theta}$, drawing each subset conditional on the value of all the others. Gibbs sampler has been widely applicable to a broad class of Bayesian analysis.

Another well-known parameter estimation method is the maximum likelihood estimation (MLE) which attempts to find the parameter values that maximize the likelihood function with given observations. However, the calculation may become complicated when the model is complicated, such as complex hierarchical models with multiple layers. MLE has ability to obtain unbiased estimators with minimum variance as the sample data carried enough information.

Compared with MLE, Bayesian is more suitable for parameter estimation with limited data due to the advantage of assigning priors. When a degradation model includes multiple layers, hierarchical Bayesian method could model the unit-to-unit variability,

conjugate prior could simplify the computation procedure if it exists, and MCMC-based simulation algorithm could obtain reasonable solutions easier.

1.3 Overview

The rest of this dissertation is organized as follows. Section 2 provides a literature review on related studies. Sections 3 and 4 state the proposed methodology and the corresponding results, respectively. Section 5 outlines three compared methods with results. Finally, Section 6 concludes this study.

CHAPTER 2: LITERATURE REVIEW

Degradation models include the general degradation-path models and stochastic processes. The relative literature review about these two categories are included in the following Section 2.1 and the Section 2.2. In addition, Bayesian degradation analysis and system degradation modeling approaches are applied in this study. Therefore, the Section 2.3 and the Section 2.4 are the literature reviews about these two topics.

2.1 General Degradation-Path Models

This section reviews studies related to the general degradation-path models, which describe the degradation-path of systems or components by using regression methods. For the regression methods, the mean regression functions are usually used to describe the expected degradation-paths, and the deviations from the mean regression functions (i.e., statistical errors) in the observed degradation data are generally considered as measurement errors. There have been numerous studies related to general degradation-path models. Nikulin *et al.* [10] presented a comprehensive overview of the advances in degradation modeling with application on reliability, survival analysis, and finance. Regression methods could be classified into two types: the linear regression method and the nonlinear regression method.

2.1.1 Linear Degradation-Path Models

One of the most popular general degradation-path models is the linear model mainly due to the easiness of the linear regression analysis. The linear regression analysis can be extended to build random-effect models and accelerated degradation models. In the random-effect models, some regression coefficients are assumed to be random from

unit to unit. In the accelerated degradation models, the degradation rate (i.e., the slope coefficient) is assumed to be dependent on the operation conditions.

Here are some examples of studies applying the linear degradation models. Freitas *et al.* [11] applied a linear degradation-path model to predict train wheels' failure-time distribution. Yu [12] proposed a linear degradation-path model with a Weibull-distributed degradation rate for analyzing an accelerated degradation test. Lu *et al.* [13] proposed a linear degradation-path model with random regression coefficients and applied it on semiconductors' degradation data. Mohammed *et al.* [14] derived the time to failure distribution from a linear degradation model and applied the method on a real laser data set. Firoozeh and Mikhail [15] applied a linear regression model with considering multiple failure measures to predict the survival function. Bagdonavicius *et al.* [16] researched on degradation analysis about the failure-time data with partial renewals and multiple competing failure modes and a non-parametric method with combining a joint linear degradation model was used in their study. Peng and Tseng [17] analyzed the degradation-path by using a general linear degradation model with considering unit-to-unit variation and the corresponding life time distribution and mean time to failure (MTTF) were derived from the degradation-path model. Dakhn *et al.* [18] applied parametric and semi-parametric estimation methods on a simple linear degradation model to predict the time to failure distribution and its percentile.

2.1.2 Nonlinear Degradation-Path Models

When the observed degradation data exhibits nonlinear patterns or no linear degradation-path models are applicable, nonlinear degradation-path models are needed.

There were some examples from real world [19] to show the necessity of incorporating a nonlinear structure into a degradation process model, such as the degradation of light-emitting diodes (LEDs). The nonlinear model could capture a better understanding of the nature degradation patterns. Bae *et al.* [20] proposed a bi-exponential degradation-path model to describe the nonlinear brightness degradation phenomenon of PDPs. The same dataset was modeled and analyzed by using a change-point degradation-path model [5]. Both studies adopted the mixed-effect modeling method to account for the unit-to-unit variability and the maximum likelihood method was applied to fit the models. Bae *et al.* [21] later developed and compared these two models within the hierarchical Bayesian framework. Another example of nonlinear degradation-path models is the two-term exponential model which is applied to describe the capacity degradation of many different types of fuel cells or batteries (i.e., direct methanol fuel cells [22], lithium-ion batteries [23]). Bae and Kvam [24] proposed a degradation model with incorporating nonlinear random coefficients to capture the nonmonotonic degradation-path for highly reliable light displays. A nonlinear degradation model with consisting of dynamic covariates [25] was used to fit a degradation-path. Due to the computation challenge by involving of nonlinear function, random effects, and shape-restricted splines, simulation method was adopted to estimate the parameters.

2.2 Stochastic Process Degradation Models

The second class of degradation models are the stochastic processes, such as Wiener process and Gamma process.

2.2.1 Wiener Process

Wiener process is a continuous-time stochastic process which is also called Brownian motion (BM) [26]. Wiener process is usually applied to describe degradation phenomena caused by wear, corrosion, and crack growth.

The Wiener process with a linear drift is the most widely used stochastic process degradation model [26]. This section first introduces the Wiener process with a linear drift as a degradation model, then reviews some recent studies on nonlinear Wiener process degradation models.

2.2.1.1 Wiener Process with a Linear Drift

Let $X(t)$ denotes the state of a unit at time t (i.e., the degradation measure at time t), the Wiener process with a linear drift assumes that $X(t)$ is modeled by

$$X(t) = \mu t + \sigma B(t) \tag{2.1}$$

where μ is the drift and σ is the diffusion coefficient. The Wiener process is characterized by the independent normal increments [26], that is

$$\Delta X(t) \sim N(\mu \Delta t, \sigma^2 \Delta t) \tag{2.2}$$

where

$$\Delta X(t) = X(t + \Delta t) - X(t) \tag{2.3}$$

and $\Delta X(t)$ is independent of $X(t)$. The normality assumption makes the Wiener process be a suitable model for nonmonotonic degradation-paths.

In Chapter 1, soft failure is mentioned which means a product is considered to have failed when its degradation level exceeds a failure threshold. In a stochastic process degradation model, the degradation may hit the threshold many times due to the noise

which is included in the model. Failure-time is defined when the process first crosses the failure threshold, called the first-hitting-time (FHT). It is well-known that the FHT distribution of the Wiener process crossing a threshold *w* obeys an inverse Gaussian distribution [26]:

$$f_T(t) = \frac{w}{\sqrt{2\pi t^3 \sigma^2}} exp\left(-\frac{(w-\mu t)^2}{2\sigma^2 t}\right) \quad (2.4)$$

Due to the availability of the closed-form FHT distribution, the Wiener process with a linear drift has been widely used in degradation modeling.

The Wiener process with a linear drift is applicable to the degradation data with linear patterns. A Wiener process with a linear drift is widely adopted on deriving FHT distribution by applying the inverse Gaussian distribution. Liu *al et.* [27] applied the Wiener process in both linear and nonlinear accelerated degradation testing analyses and compared the Wiener process with the general linear path degradation model. The simulation results showed that the reliable lifetime results could be obtained from both linear and nonlinear Wiener process models. Ye *et al.* [28] compared the Wiener process with a positive linear drift in an existing inference procedure and proposed a mixed effects model of measurement errors to improve its estimation efficiency. The proposed model was applied on the magnetic head wear problems and the light intensity degradation problems. The Wiener process with a linear drift was also adopted in the study of Tang *et al.* [29] in a mis-specification model to estimate the RUL. The related case study concluded that the mis-specification could cause premature maintenances and increase the maintenance costs. Son *et al*. [30] applied the Wiener process model in the

principal component analysis to model the components deterioration and estimate the RUL.

2.2.1.2 Wiener Process with Linearized Drift

When the degradation pattern is nonlinear, one may apply a transformation method to linearize the degradation data so that the linear Weiner process can be applied. However, deriving the life time distribution by using the FHT of a standard BM crossing a threshold cannot be applied directly in a Wiener process with a nonlinear drift. Some researchers used some transformation methods to convert the nonlinear drift to a standard BM. For example, Whitmore [31] discussed degradation modeling by applying Wiener diffusion with a time scale transformation and predicted the potential life of long-term equipment. Log-transformation method was employed by Gebraeel *et al.* [32] in a Wiener process to linearize the drift. Time scale transformation was also adopted by Doksum and Hoyland [33], Whitmore and Schenkelberg [34] to fit degradation data. Wiener process was applied by Wang *et al*. [19] with a nonlinear drift coefficient which was closer to the real degradation data and a time-space transformation was used to convert the proposed model into a standard BM. Then the concept of the FHT was borrowed to derive the closed-form of the RUL. A Wiener process with a nonlinear drift coefficient and a constant threshold was transformed by Si *et al.* [35] to a Wiener process with a linear drift and a variable threshold. The FHT of the proposed model was obtained by a time-space transformation based on a mild assumption. And the results indicated that the accuracy of the RUL estimation was improved significantly.

2.2.1.3 Wiener Process with a Nonlinear Drift

However, more and more systems' degradation characteristics cannot be captured by Wiener processes with a linear drift. To solve this problem, Wiener process with a nonlinear drift was explored by lots of researchers. Wang *et al.* [36] proposed an adaptive method of residual life (RL) estimation by applying a generalized Wiener degradation process with considering various uncertainty situations, such as the nonlinearity, and the proposed method of RL estimation could be used for future decision making and its validity was demonstrated in the case of concerning fatigue cracks. Tang *al et*. [37] considered measurement errors and applied Wiener process with nonlinear drift on real time RUL prediction to improve the accuracy of the model. Tang *et al.* [38] also introduced nonlinear Wiener process in an accelerated degradation process with random effects. Wiener process [39] was adopted in a nonlinear age and state-dependent degradation model to derive the RUL and the concept of the FHT was borrowed. An example was presented in his study to illustrate the applicability of the Wiener process model.

2.2.2 Gamma and Other Processes

Besides the Wiener process, some other popular stochastic models like Gaussian process, gammas process which are applied widely in degradation analysis.

Inverse Gaussian process was used by many researchers for degradation analysis. Peng *et al.* [40] applied a simple inverse Gaussian process model and three inverse Gaussian process models with considering random effects on the degradation analysis and applied their models on the GaAs Lasers data. In 2015, Pan *et al*. [41] estimated the

RUL via applying an inverse Gaussian degradation model. It mentioned that the RUL prediction was critical on setting the product maintenance in advance and maximizing the utilization. Wang and Xu [42] integrated the subject-to-subject heterogeneity and covariate information in a class of inverse Gaussian process models for degradation analysis. A set of laser data was used to apply those models and the corresponding failure-time distributions were derived. Peng *et al.* [43] extended the general degradation process model with constant degradation rates to parametric inverse Gaussian process models with three types of degradation rates: constant, monotonic, and S-shaped degradation rates. The degradation data of a heavy-duty machine tool's spindly system with observed time-varying degradation rates was used to test their proposed method. Pan *et al.* [44] applied expectation maximization algorithm to estimate the parameters of an inverse Gaussian model which was used to analyze the degradation of a deteriorating system with considering the random effects.

Another popular stochastic process is gamma process. A gamma process has independent gamma distributed increments which are non-negative. Geometric motion gamma process with an accelerated testing variable was applied by Park *et al.* [45] for degradation analysis. Lawless *et al.* [46] used the random effects in a gamma process to model the degradation data with considering various rates over time. Gamma process was adopted by Pan *et al.* [47] with applying two different performance measures in a degradation analysis problem. The combination of a gamma process and a Poisson process was used in the research of Noortwijk *et al.* [48] for reliability analysis with considering the random variability which was modeled via a generalized Pareto

distribution. Wang *et al.* [49] investigated Gamma processes with time transformation and random effects considered to predict the life time of an individual and the corresponding population. The accelerated degradation data of carbon-film resistors was adopted in their study to illustrate the applicableness of their proposed method. Sun *et al.* [50] combined the Arrhenius model which is a popular traditional accelerated model and the Gamma stochastic process on the reliability analysis of the accelerated aging of rubber O-rings. A comparison was included in their study to state the advantages of the improved method. Mahmoodian and Alani [51] adopted a gamma process to model the monotonic behavior of the ageing and the deteriorating processes of concrete sewer pipes and the failure probability function of the pipes caused by the corrosion process was derived from the model.

2.3 Bayesian Degradation Analysis

A proper degradation model can be used for deriving failure-time distribution, RUL of a system. Some corresponding studies of Bayesian degradation analysis are reviewed here. Bae *et al*. [52] conducted a research by applying Bayesian degradation analysis for considering competing risks and RUL prediction of two-term degradation. Ji and Yuan [53] proposed a hierarchical Bayesian degradation model for analyzing heterogeneous degradation data. They applied a Gaussian mixture model for accounting the variability of different units. Gibbs sampling was applied for estimating the parameters and a failure-time distribution was developed by using the hierarchical Bayesian degradation model for future prediction. Lee *et al.* [54] applied Bayesian degradation analysis in a bivariate Wiener process with using the censoring marker value

at the failure-time to predict its failure-time distribution. Metropolis-Hasting Gibbs sampling was adopted for estimating parameters. Another study [14] applied Bayesian degradation approach in a linear mixed model with considering grouped and non-grouped failure data to estimate the parameters of the failure-time distribution. The results showed the Bayesian approach with non-grouped data is better than the Bayesian approach with grouped data. Bayesian method [55] was applied in nonlinear degradation models by using the information from Accelerated Destructive Degradation Tests (AADTs) to estimate the precision of a failure-time distribution. A numerical example was presented to investigate the effects of the prior distribution and the sample size on test results. Peng *et al.* [40] applied Bayesian analysis and three IG process models with random effects for degradation analysis and the GaAs Lasers data was used to prove its effectiveness. Pan *et al.* [44] applied Bayesian method by using fresh degradation data to update the latest RUL estimations and make the estimations able to be real-time based.

2.4 System Degradation Modeling Approaches

As an alternative of traditional reliability modeling and prediction methods based on failure-time data, degradation analysis has attracted an increasing attention in recent years [10, 13, 56]. This section focuses on the system degradation modeling and analysis with consisting of multiple continuous-state components.

There are two general approaches applied into continuous-state system reliability analysis: black-box approach and white-box approach [6]. The biggest part of the existing degradation modeling methods is based on the black-box approach. Black-box approach [6] focus on reliability analysis on system level which assumes the system is a unit and

concentrating on the degradation testing and modeling for reliability prediction and resulting maintenance optimization at the system level. For example, Wang and Pham [57] developed a s-dependent competing risk model for systems subject to multiple degradation processes and random shocks. Liao *et al.* [58] studied continuously degrading systems based on a conditional maintenance model with a realistic maintenance limit policy. Wang and Coit [59] investigated multiple degradation measures on system degradation modeling with prediction of the system reliability. Gao *et al.* [60] developed reliability models for degradation-shock dependence systems. The Micro-Electro-Mechanical systems were used as examples in that study. Zhao *et al.* [61] optimized the warranty cost for mechanical systems under imperfect repairs using experimental degradation data of the systems. Those studies assumed that the system is a single unit with two states of functioning: working or failed.

On the other hand, while white-box approach [6] models and predicts the reliability of a system based on the system structure and the information obtained at the component level. Based on this requirement, researchers always consider the inner structure of the system and study the reliability or degradation patterns about all of the components. There have been several studies pursuing reliability prediction and maintenance optimization of systems with degrading components using the white-box approach. Those studies usually regarded the system as a binary-state system. For example, Peng *et al*. [62] investigated importance measures for the systems with independent or dependent degrading components, assuming the systems to be binary-state systems. Zhao *et al*. [63] proposed a reliability modeling and data analysis method

for load-sharing systems with identical degrading components. The degradation of a component was modeled by the Wiener process, but the system is assumed to be binary. Sun *et al.* [64] adopted the white-box approach to obtain optimal inspection and replacement policies for systems with multiple degrading components, where the systems are assumed to be binary. Nezakati *et al.* [65] considered the reliability analysis of a binary-state *k*-out-of-*n*:*F* system whose components are degrading according to a linear degradation model. Normally, it's easier to collect reliability data and other information of each individual component than the whole system. Such as connection information between two or more components, performing reliability tests on different components, abundant reliability information of components, and dependent or independent relationship among two or more components. Thus, this approach is legitimate when the system structure is complex.

There have been very limited studies on the degradation modeling of continuous-state systems with continuous-state components. Yang and Xue [66], Brunelle and Kapur [67], and Gamiz *et al*. [68] extended the binary-state reliability analysis to continuous-state reliability analysis. The system state is related to its components' states was defined via a deterministic structure function as $Y(t) = \varphi(X_1(t), X_2(t), \cdots, X_m(t)$ where $Y(t)$ and $X_i(t)$ are the state of a system and the state of the *i*th component at time *t*, respectively, and the number of components in the system is *m*. Here, $\varphi(\cdot)$ denotes the structure function from $X_i(t)$ to $Y(t)$. The structure functions may be extremely complicated for complex systems. Brunelle and Kapur [67] and Gamiz *et al*. [68] proposed some empirical methods to obtain the approximations of the structure functions.

In addition, Han and Lee [69] considered the health monitoring for a photovoltaic system, which is another example of the continuous-state system composed of continuous-state components. The degradation of solar cell modules caused the degradation of the photovoltaic system. However, that study focused on a testing method that will effectively detect the most degraded component in a system, without considering the degradation modeling and analysis. Sun *et al.* [70] studied the lifetime prediction for an integrated LED lamp, whose performance degrades as the results of the degradation of its two key components: an LED light source and a driver. Therefore, the integrated LED lamp is also an example of continuous-state systems with continuous-state components. That study, however, focused on a physics-of-failure based electronic-thermal simulation methodology for the system lifetime prediction.

Some recent studies have attempted to model and analyze degradation data of various types of fuel cells. Guida *et al.* [71] developed a random-effects models for degradation analysis of solid oxide fuel cells. The analysis was performed at the cell level to predict the cell reliability. The stack reliability was not considered in that study. On the other hand, Jouin *et al.* [72] modeled the power degradation of proton exchange membrane fuel cell stacks using stack-level measurement data. Our study, therefore, differs from those studies in that we attempt to using the cell-level degradation data to predict the stack-level reliability.

In summary, there is no study in degradation analysis about continuous-state system with continuous degradation components by using white-box approach. This research attempts to model continuous-state system's degradation and predict the failure-

time and RUL based on one of the aforementioned degradation measures. The degradation data collected from each individual cell of the monitored PEMFC stack is used to test the proposed model, mainly under the hierarchical Bayesian framework.

CHAPTER 3: PROPOSED METHODOLOGY

PEMFCs have attracted broad attentions as one of the most promising clean energy sources and the leading technology for stationary and larger vessel applications due to their high-power density, fast startup, and low pollutant emission at the point of use [3].

An industrial collaborator conducted long-term degradation tests for planar PEMFC stacks. Each stack consisted of 32 PEMFCs cells connected with series as shown in Figure 1 in Chapter 1. Under a constant power operation condition [3], the voltage behaviors of all cells in a stack are simultaneously and continuously monitored. Figure 2 depicts typical voltage degradation curves of each cell in a stack. The degradation of cell voltages causes the voltage degradation of the entire stack.

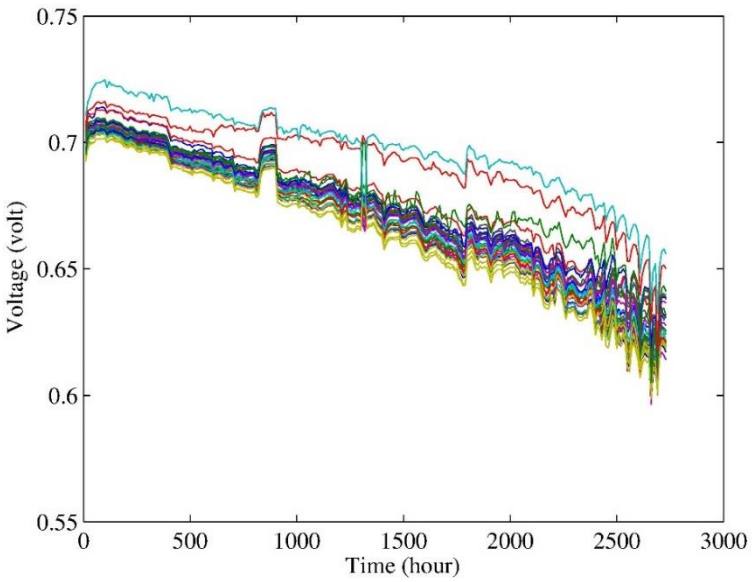

Figure 2. Observed voltage degradation-paths of 32 fuel cells in a tested PEMFC stack system [3]

A degradation-path function that has been employed to describe the capacity degradation of many different types of fuel cells or batteries (i.e., direct methanol fuel cells [22], lithium-ion batteries [23]) is the two-term exponential function. Based on this model, this study uses the two-term exponential degradation model on the data set of PEMFCs. Section 3.1 lists all assumptions of the following models. Section 3.2 introduces the two-term exponential degradation model for an individual cell. Section 3.3 gives a detail of the hierarchical Bayesian modeling approach for PEMFCs system based on the model in the Section 3.2., the failure-time distribution of a randomly selected stack and the RUL of the monitored stack are derived in the Section 3.4 based on the hierarchical Bayesian model of Section 3.3. Gibbs sampling is used to perform the Bayesian computation.

3.1 Assumptions

The proposed methodology is based on the following assumptions:

(1) The *m* fuel cells that are connected in a PEMFC stack degrade independently.

(2) The *m* fuel cells in a randomly selected stack form a random sample from the population of cells.

(3) The stack-to-stack (i.e., system-to-system) variation in degradation is caused by the cell-to-cell variation in voltage degradation. This assumption is imposed due to the availability of data for only one tested stack.

(4) A stack is considered to have failed if its output voltage falls below a failure threshold or at least *k* cells in the stack have voltages below a safety threshold. The values of the two thresholds are given in priori.

3.2 Individual Cell Degradation Model

This section presents a two-term exponential model for describing the degradation-path of an individual fuel cell. The two-term exponential model is given by

$$y_j = g(t_j; \boldsymbol{\beta}) + \varepsilon_j$$
$$= \beta_1 * \exp(\beta_2 * t_j) + \beta_3 * \exp(\beta_4 * t_j) + \varepsilon_j \quad (3.1)$$

for $j = 1, 2, \ldots, n$, where n is the number of the cells in a stack. $g(t_j; \boldsymbol{\beta})$ denotes the expected degradation-path with a set of parameters $\boldsymbol{\beta} = (\beta_1, \beta_2, \beta_3, \beta_4),\ \beta_1 < 0,\ \beta_2 > 0,\ \beta_3 > 0, \beta_4 < 0$. ε_j are the random errors which are usually assumed to be independent and identically distributed (*iid*) random variables [73] with a mean zero and a variance which is denoted by σ^2, i.e., $\varepsilon_j \sim N(0, \sigma^2)$. y_i is the degradation measure, t_j is the time and $t_j > 0$.

Based on the model (3.1), a three-stage hierarchical Bayesian model of the degradation-paths of multiple cells in a stack is presented in the next section.

3.3 Hierarchical Bayesian Modeling Approach for PEMFCs System

Based on the general Bayesian degradation-path model proposed in Section 3.2, this section presents a three-stage hierarchical Bayesian model for the degradation-paths of multiple cells in a stack. The first stage models the degradation-paths of individual cells. We assume that the observed degradation-path of each cell in the stack is described by a general degradation-path model given by

$$y_{i,j} = g(t_{i,j};\ \boldsymbol{\beta_i}) + \varepsilon_{i,j} \quad (3.2)$$

where $i = 1, \ldots, m$, m is the total number of the cells in a PEMFCs system. $j = 1, \ldots, n_i$, n_i is the total number of the measurements of the ith cell. Thus, $y_{i,j}$ is the jth observation of

the *i*th cell and $t_{i,j}$ denotes the measure time of the response $y_{i,j}$. The nonlinear function $g(t_{i,j};\ \boldsymbol{\beta_i})$ denotes the expected degradation-path of the *i*th cell and the deviation terms $\varepsilon_{i,j}$ are the random errors of the cell *i* which are usually assumed to be independent and identically distributed (*iid*) random variables, i.e., $\varepsilon_{ij} \sim N(0, {\sigma_i}^2)$.

As shown in Figure 2, the observed cell degradation-paths exhibit a nonlinear pattern, showing a slower degradation phase followed by a more rapid degradation phase. Similar two-phase degradation patterns have been observed for other types of fuel cells and batteries [22, 23]. A degradation-path function that has been frequently employed to describe capacity degradation of many different types of fuel cells or batteries (i.e., direct methanol fuel cells [22] lithium-ion batteries [23]) is the two-term exponential (or called bi-exponential) function given by

$$g(t_{i,j};\ \boldsymbol{\beta_i}) = \beta_{i1} * \exp(\beta_{i2} * t_{i,j}) + \beta_{i3} * \exp(\beta_{i4} * t_{i,j}) \tag{3.3}$$

for $\boldsymbol{\beta_i} = (\beta_{i1}, \beta_{i2}, \beta_{i3}, \beta_{i4})$. He *et al*. [23] adopted the two-term exponential function to analyze the capacity degradation of lithium-ion batteries. The capacity degradation of a lithium-ion battery is closely related to the increase of its internal impedance and the sum of exponential functions has been used to model the internal impedance increase. Models based on the sum of exponential functions hence are potential for describing the capacity degradation. Bae *et al*. [22] derived the bi-exponential capacity degradation model for direct methanol fuel cells based on the second-order kinetics, considering two heterogeneous compounds existing in membrane electrode assemblies. Thus, this study adopts this two-term exponential function to model the actual degradation-path of a fuel cell due to its connection to the degradation mechanisms and good fit to the data. In

addition, more than two terms exponential function may be needed to be considered if the current two-term exponential function could not fit the degradation pattern adequately. An alternative function to describe the two-phase nonlinear degradation patterns is the change-point regression analysis, which will be discussed in Chapter 5 as an alternative model.

The second stage accounts for the cell-to-cell variation in the stack. The degradation-path parameter vectors $\boldsymbol{\beta_i}$ are assumed to form a random sample from a common multivariate distribution whose probability density function is denoted by $f(\boldsymbol{\beta}|\boldsymbol{\theta})$, where $\boldsymbol{\theta}$ denotes the parameter vector of the multivariate distribution. The multivariate normal distribution has been commonly adopted to describe the unit-to-unit variation in the literature of random-effect models and hierarchical Bayesian models. We choose a truncated multivariate normal distribution as the second stage model, namely

$$\boldsymbol{\beta} \sim MVN_4(\boldsymbol{\mu}, \Sigma) I_{\{\beta_1<0,\, \beta_2>0,\, \beta_3>0,\, \beta_4<0\}} \tag{3.4}$$

for $\boldsymbol{\theta} = (\boldsymbol{\mu}, \Sigma)$, where μ is the mean vector, and Σ is the variance-covariance matrix. Herein MVN_4 represents the multivariate normal distribution for the 4-dimensional random vector $\boldsymbol{\beta}$, and I denotes the indicator function. The distribution is restricted to the region $I_{\{\beta_1<0,\, \beta_2>0,\, \beta_3>0,\, \beta_4<0\}}$ in order to yield the observed shape of the degradation curves.

The last but not least important stage is setting prior distributions to the parameters $\boldsymbol{\mu}$, $\sum$, and σ^2 to complete the model. Due to our lack of prior knowledges, non-informative priors are employed. We also need to take the computational convenience into account when choosing the prior distributions. For the variance

parameter σ^2, we choose the conjugate Gamma prior distribution with shape parameter a and scale parameter b (i.e., $G(a,b)$) for the precision parameter σ^{-2} (i.e., the inverse of variance), where the Gamma probability density function has the form of $\frac{b^a}{\Gamma(a)}x^{a-1}e^{-bx}$, where $\Gamma(a)$ denotes the Gamma function. This is equivalent to assume the conjugate inverse-Gamma prior for the variance parameter σ^2. In Bayesian statistics, the conjugate prior of the mean vector $\boldsymbol{\mu}$ is another multivariate normal distribution, $MVN_v(\mathrm{C},\mathrm{V})$, with the mean vector C and the variance-covariance matrix V. C and V are called hyper-parameters as they are the parameters of the prior distribution for parameter $\boldsymbol{\mu}$. Here v = 4 is the length of the vector β. $MVN_v(0_v, 10^6\mathrm{I}_v)$ is chosen as a non-informative prior, where 0_v and I_v are the zero vector of length v and the $(v \times v)$ identity matrix, respectively. The conjugate prior of the covariance matrix $\sum$ is an inverse-Wishart (*IW*) distribution [74]. The probability density function of the *IW* distribution is:

$$f(\sum|\rho,\boldsymbol{S}) = \left[2^{\rho v/2}\pi^{v(v-1)/4}\prod_{i=1}^{v}\Gamma\left(\frac{\rho+1-i}{2}\right)\right]^{-1} \times$$

$$|\boldsymbol{S}|^{\rho/2}|\sum|^{-(v+\rho+1)/2}\, exp\left[-\frac{1}{2}tr(\boldsymbol{S\Sigma}^{-1})\right] \qquad (3.5)$$

where $\sum$ is a $(v \times v)$ symmetric positive-definite random matrix, ρ is the degree of the freedom, and $\boldsymbol{S}$ is a $(v \times v)$ symmetric positive-definite scale matrix. Based on this function, it's hard to set a prior distribution directly to the matrix $\sum$. Lots of studies decomposed the variance-covariance matrix into variance and correlation components as [62] $\sum = \boldsymbol{\Delta Q \Delta}$, where $\boldsymbol{\Delta} = diag(\delta_1, \ldots, \delta_v)$ is the diagonal matrix with *i*th element $\delta_i > 0$, $\boldsymbol{Q}$ is a $(v \times v)$ symmetric positive-definite matrix. Next, we assume an independent gamma prior $g(a_\delta, b_\delta)$ for δ_i, for i =1, …, v, and an inverse-Wishart prior $IW(\rho, S)$ for

the matrix $\boldsymbol{Q}$. Herein ρ is the degrees of freedom for the inverse-Wishart distribution, S is a $(v \times v)$ symmetric positive-definite matrix, a_δ and b_δ are the shape and scale parameters of the gamma prior, respectively. Assuming $G(1, 0.0001)$ and $IW\,(v + 1, \mathbf{I}_v)$ for the corresponding parameters results in a non-informative prior for the variance-covariance matrix $\sum$. Note that prior distributions are subjective and should actually reflect one's prior knowledge on the unknown model parameters. Therefore, different analysts may assume and employ different prior distributions. The non-informative prior distributions discussed in this paragraph can adequately represent the situation where we do not have any prior knowledge on the model parameters.

Given the observed cell degradation data in a stack $y \equiv \{(y_{ij}, t_{ij}): i = 1, 2, \dots, m,$ $j = 1,2, \dots, n_i\}$, the joint posterior distribution of all model parameters can be derived according to the Bayes' theorem as

$$
\begin{aligned}
&f(\boldsymbol{\beta}_1, \dots, \boldsymbol{\beta}_m, \boldsymbol{\mu}, \boldsymbol{Q}, \delta_1, \dots, \delta_v, \sigma^2 \mid d) \\
&\quad \propto f(\boldsymbol{d} \mid \boldsymbol{\beta}_1, \dots, \boldsymbol{\beta}_m, \boldsymbol{\mu}, \boldsymbol{Q}, \delta_1, \dots, \delta_v, \sigma^2) f(\boldsymbol{\beta}_1, \dots, \boldsymbol{\beta}_m) f(\boldsymbol{\mu}) f(\boldsymbol{Q}) f(\delta_1, \dots, \delta_v) f(\sigma^2) \\
&\quad \propto \prod_{i=1}^{m} \frac{1}{\sigma^{n_i}} exp\left[-\frac{(\boldsymbol{y}_i - \boldsymbol{X}_i(\gamma_i)\vartheta_i)'(\boldsymbol{y}_i - \boldsymbol{X}_i(\gamma_i)\vartheta_i)}{2\sigma^2} \right] I_{\{\beta_{1i}<0,\, \beta_{2i}>0,\, \beta_{3i}>0,\, \beta_{4i}<0\}} \\
&\qquad \times \left[P\left(\boldsymbol{\mu}, \sum \quad \right) \right]^{-m} |\boldsymbol{\Delta}|^{-m/2} |\boldsymbol{Q}|^{-m/2} |\boldsymbol{\Delta}|^{-m/2} \\
&\qquad \times exp\left[-\frac{\sum_{i=1}^{m} (\boldsymbol{\theta}_i - \boldsymbol{\mu})' \boldsymbol{\Delta}^{-1} \boldsymbol{Q}^{-1} \boldsymbol{\Delta}^{-1} (\boldsymbol{\theta}_i - \boldsymbol{\mu})}{2} \right] \\
&\qquad \times exp\left[-\frac{(\boldsymbol{\mu} - \boldsymbol{\mu}_\mu)' \boldsymbol{\Sigma}_\mu^{-1} (\boldsymbol{\mu} - \boldsymbol{\mu}_\mu)}{2} \right] \times |\boldsymbol{Q}|^{-(v+\rho+1)/2} \times exp\left[-\frac{1}{2} tr(\boldsymbol{S}\boldsymbol{Q}^{-1}) \right] \\
&\qquad \times \prod_{i=1}^{v} \delta_i^{a_\delta - 1}\, exp(-b_\delta \delta_i) \times (\sigma^2)^{-(a_\sigma + 1)}\, exp\left(-\frac{b_\sigma}{\sigma^2}\right), \qquad (3.6)
\end{aligned}
$$

where $\phi(\cdot)$ denotes the probability density function of the standard normal distribution. From the joint posterior distribution, the marginal posterior distribution $f(\boldsymbol{\theta}|\boldsymbol{y})$, $f(\sigma^2|\boldsymbol{y})$, and $f(\boldsymbol{\beta_i}|\boldsymbol{y})$, for $i = 1, 2, \ldots, m$, can be obtained. However, these marginal posterior distributions may have no closed-form expressions due to the model complexity. MCMC simulation-based algorithms, especially, the Gibbs sampling method [7, 73, 75] can be adopted to effectively obtain random samples from the marginal posterior distributions. Then, the posterior inference on the model parameters and any functions of the model parameters can be formulated by using the sample statistics. The WinBUGS software package [76, 77] is employed to perform the posterior simulation and computation in this work. All details of estimating the parameters and the corresponding steps are shown in Appendix A.

As mentioned in Chapter 2, MLE can handle this nonlinear case but it is difficult and complex in computation. However, some other potential algorithms could be compared and discussed except the MCMC simulation-based algorithm. A comparison of the most popular parametric estimation methods with discussing their advantages and weaknesses was concluded by Pinhero and Bates [78], such as the linear mixed-effects approximation and the Gaussian quadrature appropriation. Thus, their study could be used as one of the references for exploring other potential algorithms in the future.

3.4 Deviation of the RUL and the Failure-Time Distribution

The hierarchical Bayesian two-term exponential model is proposed in Section 3.3, this section will discuss the failure-time distribution of a fuel cell stack that is randomly selected from its population and the RUL of the monitored fuel cell stack based on the

proposed degradation models. *R(t)* denotes the reliability of no failure before time *t*, thus, *F(t)*= 1-*R(t*) denotes the failure-time distribution. RUL is the remaining useful life time left on a system or a component at a particular time of operation.

A PEMFC stack is composed of *m* fuel cells. The stack system degrades as the stack components degrade over time. Therefore, the system is regarded as rather a continuous-state system than a binary-state system in this study. The system is considered to fail if one or a few degradation measures are below a predefined failure threshold. Here, we consider two degradation measures for the fuel cell stack system. The first degradation measure is the overall stack output voltage, and the second degradation measure is the minimum voltage of individual cells.

A system performance is evaluated through the stack output voltage. Due to the serial configuration of the *m* cells in the stack, the stack output voltage is simply the sum of the output voltages of individual cells. Thus, the degradation of individual cell voltages results in the degradation of stack output voltage. With respect to the first degradation measure based on individual degradation-paths, the stack output voltage is given by

$$\eta_{s,1}(t;\boldsymbol{\beta}_1,\boldsymbol{\beta}_2,\dots,\boldsymbol{\beta}_m) = \sum_{i=1}^{m} g(t;\boldsymbol{\beta}_i) \tag{3.7}$$

Hereafter, the subscript *s* denotes the system-level degradation measures. The failure-time of the system based on the stack output voltage, denoted by $T_{s,1}$, is defined as the time when the degradation-path reaches or exceeds the critical threshold level $\eta_{f,1}$, i.e.,

$$T_{s,1} = \inf\{t > 0; \eta_{s,1}(t;\boldsymbol{\beta}_1,\boldsymbol{\beta}_2,\dots,\boldsymbol{\beta}_m) \leq \eta_{f,1}\} \tag{3.8}$$

The minimum cell voltage is employed as a safety measure. Whenever *k*-out-of-*m* individual cells' voltages drop below a safety threshold, the stack must be emergently shut down to prevent critical damages to the stack system [3]. As actual degradation-paths for the second degradation measure, the *k*th minimum cell voltage is defined as

$$\eta_{s,2}(t;\boldsymbol{\beta}_1,\boldsymbol{\beta}_2,\dots,\boldsymbol{\beta}_m) = min_k\{g(t;\boldsymbol{\beta}_1), g(t;\boldsymbol{\beta}_2),\dots, g(t;\boldsymbol{\beta}_m)\} \tag{3.9}$$

where $min_k\{\}$ denotes the *k*th minimum of a set. The second degradation measure actually corresponds to a *k*-out-of-*m*:*F* system. The failure-time based on the minimum cell voltage for individual cells, denoted by $T_{s,2}$, is defined as

$$T_{s,2} = \inf\{t > 0; \eta_{s,2}(t;\boldsymbol{\beta}_1,\boldsymbol{\beta}_2,\dots,\boldsymbol{\beta}_m) \le \eta_{f,2}\} \tag{3.10}$$

That is, for the failure-times of the components of a *k*-out-of-*m*:*F* system, T_1, ..., T_m, denote the corresponding order statistics by $T_{1,m} < \cdots < T_{m,m}$, then the failure-time of the *k*-out-of-*m*:*F* system is given by $T_{k,m}$.

Based on the two measurements above, the failure-time distribution and the RUL are discussed in the following two subsections.

3.4.1 Failure-Time Distribution of a Random Stack

Because only one stack was tested in the experiment owing to high testing cost and the restriction of testing equipment, we made the assumption that stack-to-stack variation is mainly due to the cell-to-cell variation. Let a continuous random variable T_s denotes the time-to-failure of a randomly selected stack. A stack is considered to have failed if one of the two degradation measures falls below the corresponding threshold first such that $T_s \equiv min\{T_{s,1}, T_{s,2}\}$. Using the hierarchical Bayesian degradation model

presented in Section 3.3 and conditioning on a given $\boldsymbol{\theta}$ vector, the failure probability at a mission time *t* of a random stack is defined as

$$\begin{aligned} F_s(t|\boldsymbol{\theta}) &= Pr(T_s < t|\boldsymbol{\theta}) \\ &= \int \dots \int \Pr[\{h_{s,1}(t;\boldsymbol{\beta}_1,\dots,\boldsymbol{\beta}_m) \le \eta_{f,1} \cup h_{s,2}(t;\boldsymbol{\beta}_1,\dots,\boldsymbol{\beta}_m) \le \\ &\quad \eta_{f,2}\}] \prod_{i=1}^{m} f(\beta_i/\boldsymbol{\theta}) d\boldsymbol{\beta}_1 \dots d\boldsymbol{\beta}_m \end{aligned} \tag{3.11}$$

The $\boldsymbol{\theta}$ vector is a random vector whose posterior distribution is denoted by $f(\boldsymbol{\theta}|\boldsymbol{y})$. We can derive the posterior distribution of the failure-time distribution $F_S(t)$, i.e., $f(F_s(t|\boldsymbol{y}))$, via the transformation of random variables. Because of the complexity of the model, $f(F_s(t|\boldsymbol{y}))$ does not have a closed-form expression. An MCMC simulation-based algorithm is employed to estimate the posterior distribution of the failure-time distribution $f(F_s(t|\boldsymbol{y}))$ in this study. The algorithm is briefly outlined below:

Step 1: Simulate *N* $\boldsymbol{\theta}$ vectors from the marginal posterior distribution $f(\boldsymbol{\theta}|\boldsymbol{y})$. This can be accomplished using the Gibbs sampling algorithm.

Step 2: For each $\boldsymbol{\theta}$ vector obtained in Step 1, simulate *L* random stacks. A random stack is obtained by simulating *m* random cells whose degradation-path parameter vectors (i.e., $\boldsymbol{\beta}_1, \boldsymbol{\beta}_2 \dots, \boldsymbol{\beta}_m$) are randomly drawn from $f(\boldsymbol{\beta}|\boldsymbol{\theta})$. Basically, a random stack is generated by randomly simulating *m* cells from the population of cells. Then calculate the failure fraction of the simulated random stacks that have failed by time *t* according to the two threshold values.

Step 3: The failure fractions obtained in Step 2 for all *N* simulated $\boldsymbol{\theta}$ vectors form a random sample from the posterior distribution $f(F_s(t|\boldsymbol{y}))$. Then, posterior inference on $F_s(t)$ can be obtained using the sample statistics. Especially, this dissertation uses sample

medians as point estimates, and formulated interval estimated using the 2.5^{th} and 97.5^{th} sample percentiles.

One may derive the stack failure-time distribution via only one of the two degradation measures. Conditioning on a given $\boldsymbol{\theta}$ vector, the failure-time distribution based on the stack output voltage measure only is defined as

$$F_{s,1}(t|\boldsymbol{\theta}) = \int \dots \int [\Pr\left(h_{s,1}(t;\boldsymbol{\beta}_1,\dots,\boldsymbol{\beta}_m) \le \eta_{f,1}\right)) \times \prod_{i=1}^{m} f(\beta_i/\boldsymbol{\theta}) d\boldsymbol{\beta}_1 \dots d\boldsymbol{\beta}_m \quad (3.12)$$

Similarly, the failure-time distribution based on the minimum cell voltage measure only is given by

$$F_{s,2}(t|\boldsymbol{\theta}) = \int \dots \int [\Pr\left(h_{s,2}(t;\boldsymbol{\beta}_1,\dots,\boldsymbol{\beta}_m) \le \eta_{f,2}\right)) \times \prod_{i=1}^{m} f(\beta_i/\boldsymbol{\theta}) d\boldsymbol{\beta}_1 \dots d\boldsymbol{\beta}_m \quad (3.13)$$

Because the two degradation measures $h_{s,1}(t;\boldsymbol{\beta}_1,\dots,\boldsymbol{\beta}_m)$ and $h_{s,2}(t;\boldsymbol{\beta}_1,\dots,\boldsymbol{\beta}_m)$ are defined based on the same set of cell degradation-path, the two degradation measures may be dependent. However, if the two degradation measures are assumed to be independent, then

$$\begin{aligned} &\Pr(\{h_{s,1}(t;\boldsymbol{\beta}_1,\dots,\boldsymbol{\beta}_m) \le \eta_{f,1}\} \cup \{h_{s,2}(t;\boldsymbol{\beta}_1,\dots,\boldsymbol{\beta}_m) \le \eta_{f,2}\}) \\ &= 1 - \Pr(\{h_{s,1}(t;\boldsymbol{\beta}_1,\dots,\boldsymbol{\beta}_m) > \eta_{f,1}\} \cap \{h_{s,2}(t;\boldsymbol{\beta}_1,\dots,\boldsymbol{\beta}_m) > \eta_{f,2}\}) \\ &= 1 - \Pr(\{h_{s,1}(t;\boldsymbol{\beta}_1,\dots,\boldsymbol{\beta}_m) > \eta_{f,1}\} \times \{h_{s,2}(t;\boldsymbol{\beta}_1,\dots,\boldsymbol{\beta}_m) > \eta_{f,2}\}), \end{aligned} \quad (3.14)$$

where the first equality is based on the DeMorgan's Laws in probability and the second equality is the result of the independence assumption. Under the independence assumption the stack failure-time distribution would, then, be predicted by

$$F_s^{ind}(t|\boldsymbol{\theta}) = \int \dots \int [1 - \Pr(h_{s,1}(t; \boldsymbol{\beta}_1, \dots, \boldsymbol{\beta}_m) > \eta_{f,1}) \times \Pr(h_{s,2}(t; \boldsymbol{\beta}_1, \dots, \boldsymbol{\beta}_m) > \eta_{f,2}) \times \prod_{i=1}^{m} f(\beta_i/\boldsymbol{\theta})] d\boldsymbol{\beta}_1 \dots d\boldsymbol{\beta}_m. \quad (3.15)$$

By comparing the $F_s(t)$ and $F_s^{ind}(t)$, we may empirically evaluate the independence between the two degradation measures.

3.4.2 RUL of the Monitored Stack

Given a time t_c which denotes the monitored stack is already worked for a time t_c and the current observed cells' degradations $\boldsymbol{d}_c \equiv (y_{ij}, i = 1, \dots, m; j = 1, \dots, n_i)$, then the remaining time can be predicted until the system failed. Let t_R denotes the RUL of the monitored system at time t_c, $\boldsymbol{\beta}_i$(i =1, …, m) is the parameter set of the ith cell of the stack. Then the RUL of the monitored stack is defined as:

$$t_R \equiv min(t_{R,1}, t_{R,2}) \quad (3.16)$$

where $t_{R,i} = \inf\{t \geq 0; \eta_{s,i}(t_c + t_i; \boldsymbol{\beta}_1, \dots, \boldsymbol{\beta}_m) \leq \eta_{f,i}\}, i = 1, 2$. For the computation, an MCMC simulation-based algorithm is employed to estimate the posterior median of the RUL. Suppose that μ, Σ, and σ^2 are already simulated from the Section 3.3. Then generate many estimating values of $\boldsymbol{\beta}$ from the function (3.6) which is extended from the research [51]. Suppose the number of the simulated $\boldsymbol{\beta}$ is L, then for each set of β_l, compute the related degradation value of each cell. Finally, apply the function (3.16) to predict the posterior median of the RUL.

CHAPTER 4: RESULTS

In the Chapter 3, the hierarchical Bayesian degradation model was presented, and the failure-time and RUL were discussed. The MCMC-based simulation algorithm was adopted to estimate the parameters of the models. The corresponding results are presented in this chapter. The Section 4.1 states all parameters initial settings for the MCMC simulation algorithm and the results of the hierarchical degradation model. The estimated results of the failure-time distribution and RUL are concluded in Section 4.2 with discussions.

4.1 Hierarchical Degradation Modeling

In the degradation analysis for the PEMFC stack system, we first fitted the hierarchical Bayesian degradation model presented in Section 3.3. For the function (3.6), set a non-informative initial for $\boldsymbol{\mu}$ = (0, 0, 0, 0)'. $\boldsymbol{\Sigma} = \boldsymbol{\Delta Q \Delta}$, where $\boldsymbol{\Delta} = diag(\delta_1, \ldots, \delta_v)$ is the diagonal matrix with $\delta_i > 0$, and $\boldsymbol{Q}$ has the IW prior with degree of freedom $\rho = v + 1$ and a $v \times v$ symmetric positive-definite scale matrix $\boldsymbol{S}$. Thus, $\boldsymbol{\Delta} = diag(1, 1, 1, 1)$, $\delta_i \sim g(1, 0.0001)$, $\boldsymbol{Q} \sim IW(4, I_4)$, and ρ =5. For the error terms in the formulas (3.2) and (3.6), assume the precision parameter σ^{-2} have gamma prior with parameters a and b, i.e., $\sigma^{-2} \sim G(a, b)$. To reflect the non-informative of the prior, set a = 1 and b = 0.001 which result in a very flat shape of the distribution. Gibbs sampling is applied for the computation in WinBUGs. Thus, more than two terms exponential degradation-path function does not need to be discussed here.

Table A summarizes the parameters' posterior medians for 32 individual cells of the Bayesian two-term exponential degradation model. For example, Figure 3 plots the posterior median of the predicted actual degradation-path for fuel cell #1. From this figure, we could see that the two-term exponential degradation-path function provides a reasonable fit to the observed cell voltage degradation. Thus, more than two terms exponential degradation-path function does not need to be discussed here.

Table A Posterior medians of the parameters in the two-term exponential degradation-path function

Cell #, i	$\beta_{i1}(\times 10^{-5})$	β_{i2}	β_{i3}	$\beta_{i4}(\times 10^{-2})$
1	-1.18	2.945	0.7129	-3.691
2	-1.41	2.835	0.709	-3.643
3	-1.21	2.852	0.7086	-3.85
4	-1.27	2.852	0.7083	-3.645
5	-6.46	3.061	0.7062	-3.904
6	-1.28	2.828	0.7083	-3.919
7	-1.34	2.797	0.7085	-3.559
8	-1.39	2.749	0.7068	-4.054
9	-1.31	2.796	0.706	-3.681
10	-1.36	2.758	0.7135	-3.348
11	-1.67	2.661	0.7057	-3.923
12	-1.46	2.667	0.7054	-3.895
13	-1.59	2.666	0.7038	-4.062
14	-1.77	2.565	0.7053	-3.985
15	-1.64	2.651	0.7111	-3.747
16	-1.42	2.712	0.7064	-3.699
17	-1.94	2.331	0.71	-3.647
18	-2.24	2.204	0.7066	-3.677
19	-1.51	2.486	0.7081	-3.543
20	-1.65	2.564	0.7044	-4.198
21	-1.91	2.309	0.7102	-3.759
22	-1.45	2.659	0.7096	-3.734
23	-1.38	2.642	0.7107	-3.664
24	-1.28	2.747	0.7071	-3.853
25	-1.26	2.733	0.7074	-3.718
26	-9.96	2.813	0.7078	-3.563
27	-1.12	2.784	0.7047	-3.876
28	-9.89	2.902	0.7075	-3.132
29	-1.36	2.544	0.7068	-3.23
30	-1.51	3.586	0.706	-2.659
31	-8.92	3.083	0.7152	-1.933
32	-2.07	3.55	0.721	-2.092

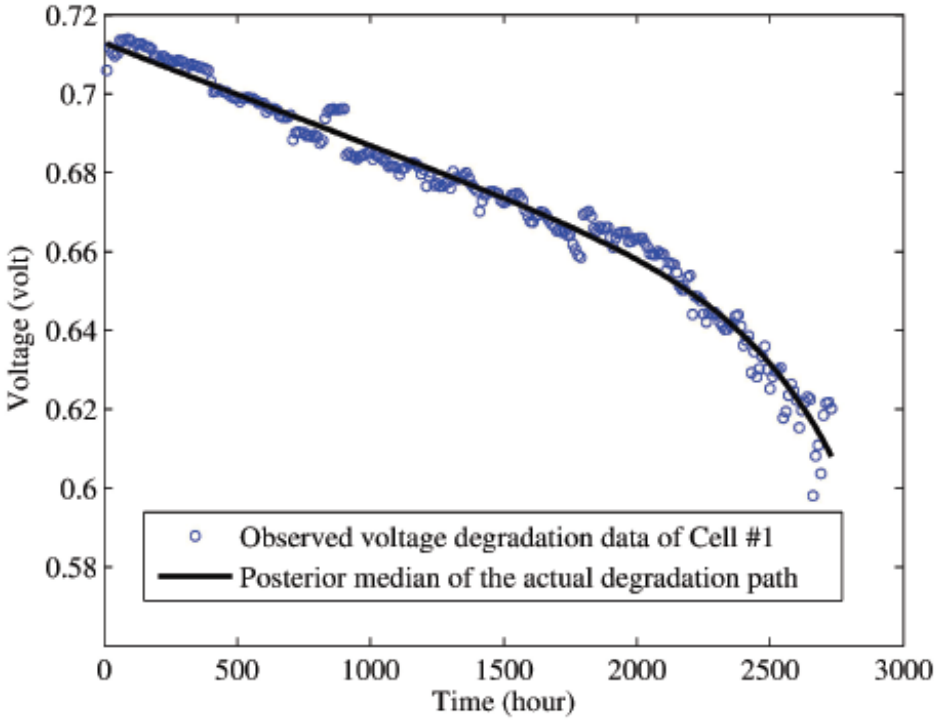

Figure 3. Posterior median fit to the degradation-path for fuel cell #1

4.2 Failure-Time Distribution and RUL

In the Section 3.4, the failure-time distribution of a fuel cell stack that is randomly selected from its population and the RUL of the monitored fuel cell stack are discussed. Based on the parameters' estimations from Section 4.1, Gibbs sampling is used for computing the degradation data in this part. From above discussion, two types of performance measures are used for deriving the failure-time distributions $F_s(t)$, $F_s^{ind}(t)$, and the RUL.

4.2.1 Failure-Time Distribution

In this section, we assume that a PEMFC stack is considered to have failed if its actual output voltage is below 20 *V* or at least *k* cells in the stack drop below a safety threshold of 0.6 *V*, which one comes first. In Section 3.4, two failure-time distributions

(3.11) and (3.15) are derived: the failure time distribution $F_s(t)$ is obtained from the hierarchical Bayesian degradation model directly, and the other one $F_s^{ind}(t)$ which is derived based on the independence assumption of the two degradation measurements.

Figure 4 plots the posterior medians of the failure time distribution based on the performance measure $F_{s,1}(t)$, and the failure-time distribution based on the safety measure $F_{s,2}(t)$ for k = 1, 2, 3. Two degradation measures overlap and the two failure modes compete together to determine the overall failure-time distribution of a random stack. As k increases, the failure mode due to the first performance degradation $F_{s,1}(t)$ becomes more dominating.

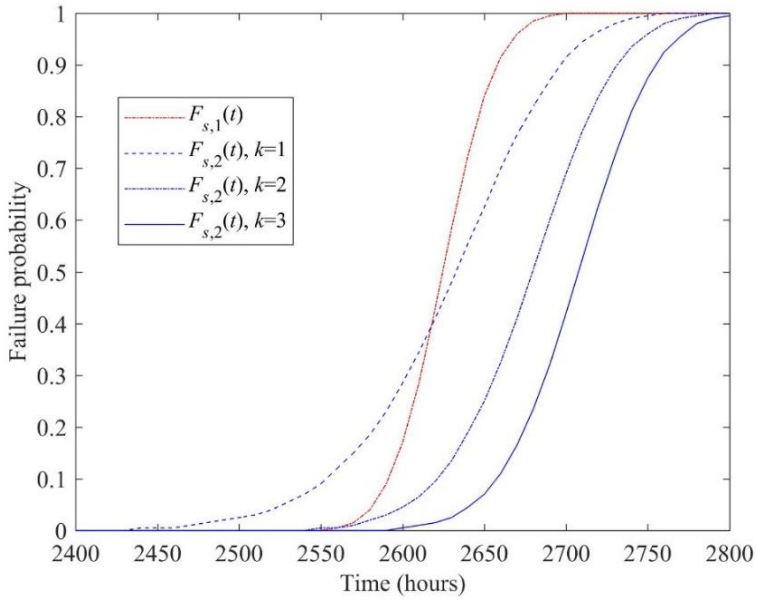

Figure 4. Posterior median estimation of $F_{s,1}(t)$, and $F_{s,2}(t)$ for k = 1, 2, 3

Figure 5 and Figure 6 show the posterior medians of $F_{s,1}(t)$, $F_{s,2}(t)$, $F_s(t)$, and $F_s^{ind}(t)$ for k = 1 and 2, respectively. Note that there is no significant difference between

$F_s(t)$ and $F_s^{ind}(t)$**,** implying that the two degradation measures may be independent. However, we are not able to prove the independence between the two degradation measures, and the above statement on the independence is obtained empirically by comparing the results from Equations (3.11) and (3.15). Moreover, by comparing the posterior medians of $F_s(t)$ for k = 1 in the Figure 5 and k = 2 in the

Figure 6, the safety degradation measure plays a more important role for determining the overall stack failure at the earlier phase of the operation. As operation time increases, the performance degradation measure becomes more dominating.

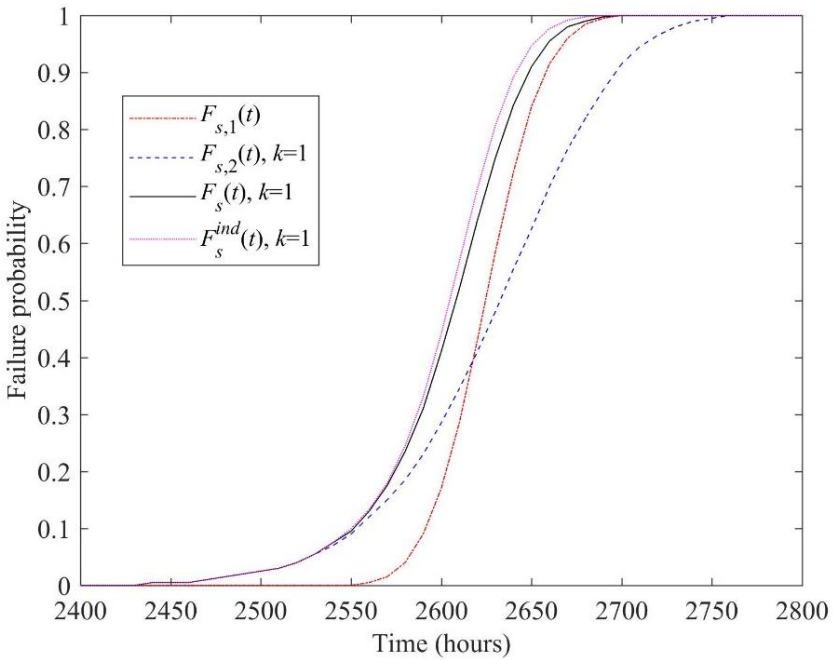

Figure 5. Posterior medians of $F_{s,1}(t)$, $F_{s,2}(t)$, $F_s(t)$, and $F_s^{ind}(t)$ (k = 1)

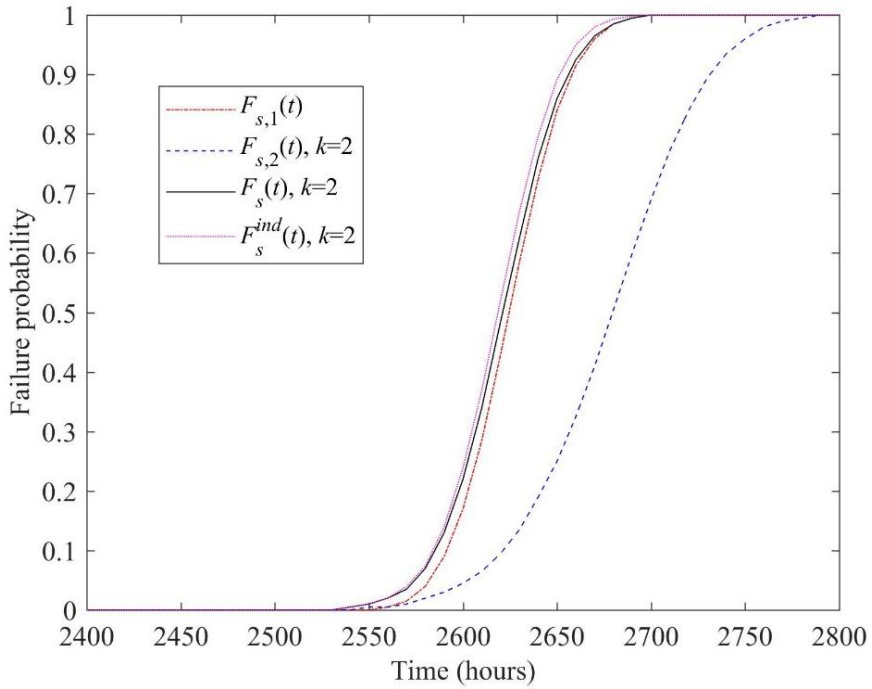

Figure 6. Posterior medians of $F_{s,1}(t)$, $F_{s,2}(t)$, $F_s(t)$, and $F_s^{ind}(t)$ (k = 2)

For current stack under study, we also obtain the posterior estimates of its failure-time summarized in Table B. The failure-time, T_s of the stack is determined by the performance measure, that is, $T_s \equiv min(T_{s,1}, T_{s,2}) = T_{s,1}$, where $T_{s,1}$ is the posterior estimate failure-time based on the performance measure, and $T_{s,2}$ is the posterior estimate failure-time based on the safety measure.

Table B Posterior estimates medians and 95% Bayesian intervals (in parentheses) of the failure-time (hours) for the stack under study

k	T_s	$T_{s,1}$	$T_{s,2}$
k=1	2654.2 (2650.8, 2657.8)	2654.2 (2650.8, 2657.8)	2780.9 (2764.4, 2794.9)
k=2	2654.2 (2650.8, 2657.8)		2788.4 (2775.2, 2800.8)
k=3	2654.2 (2650.8, 2657.8)		2793.9 (2781.8, 2806.1)

4.2.2 RUL

In this section, two sets of thresholds are used to estimate the posterior RUL based on the Equation (3.16). Under the first set of the thresholds, given $t_c = 2730$ hours, $\eta_{f,1}$= 20 *V*, and $\eta_{f,2} = 0.6$ *V*, Table C shows the posterior estimates of the RUL of the current stack with *k* = 1, 2, 3. We could see that the current stack already failed under the performance measure with the threshold 20 *V*. However, the cell's degradation based on the safety measure still can be tested due to the specialty of soft failure.

Table C Posterior estimates medians and 95% Bayesian intervals with thresholds 20 *V* and 0.6 *V*

k	T_R	$T_{R,1}$	$T_{R,2}$
k=1	0	0	50.9 (34.4, 64.9)
k=2	0		58.4 (45.2, 70.8)
k=3	0		63.9 (51.8, 76.1)

For the second set of thresholds, given $t_c = 2730$ hours, $\eta_{f,1}$= 17.5 *V*, and $\eta_{f,2} =$ 0.5 *V*. Table D shows the posterior estimates of the RUL of the current stack with *k* = 1, 2, 3.

Table D Posterior estimates medians and 95% Bayesian intervals with thresholds 17.5 *V* and 0.5 *V*

k	T_R	$T_{R,1}$	$T_{R,2}$
k=1	428.3 (388.5, 457.7)	447.0 (426.9, 466.7)	428.5 (388.5, 464.4)
k=2	443.0 (411.4, 464.4)		448.4 (411.5, 482.0)
k=3	446.3 (424.0, 466.3)		462.5 (428.0, 494.1)

From above results, we could conclude that the values of thresholds are critical for predicting the RUL of the monitored stack. When the thresholds $\eta_{f,1}$= 20 *V* and

$\eta_{f,2} = 0.6\ V$, the RUL of the stack is determined by the overall stack voltage. While the set of the thresholds $\eta_{f,1}$= 17.2 *V* and $\eta_{f,2} = 0.5V$ are used to define the fuel stack failure, the performance measure becomes more dominating for estimating the RUL as *k* increases.

In summary, above results illustrate that the proposed two-term exponential degradation-path model is reasonable to describe the degradation-path of the fuel cell stack. And the corresponding derived failure-time distribution and RUL are acceptable. The failure time distributions estimations noted that the two degradation measures may be independent but there is no physical evidence to prove that. For the safety measure, we use at least *k* cells voltages below the threshold to define the failure and the value of *k* impact the predication results. Moreover, the thresholds values are critical to determine the fuel cell stack failure and different thresholds sets could lead totally different estimation results. In the following chapter, three alternative methods are adopted to this data set for comparison.

CHAPTER 5: COMPARISON METHODS

The results presented in the previous chapter indicated that the proposed two-term exponential degradation-path model is reasonable to analyze the fuel cell stack data set. The remaining research tasks focus on exploring and comparing alternative methods with corresponding results.

5.1 Degradation Analysis with Only Considering Safety Measurement

Bae *et al.* [3] considered the safety measure only in their previous study, then applied an approximate degradation analysis to find out the stack reliability. Their approach took the following four steps: first, they fitted the 32 cells degradation-paths using some nonparametric smoothing method. Second, they extrapolated the smoothed degradation curves to the failure threshold $\eta_{f,2} = 0.6\,V$ to obtain the failure-times for 32 fuel cells. Third, they fitted a parametric distribution to the failure-times obtained in the previous step by assuming that they form a random sample of cell failure-times. Finally, the stack failure-time distribution corresponds to the distribution of the *k*th order statistics was concluded. Following their approach, we performed the following analysis as an alternative and made a comparison with the proposed approach. By considering the minimum cell voltage measure only, the stack is actually a *k*-out-of-*m*:*F* binary-state system. Using the hierarchical Bayesian model for cell degradation, we can derive the failure-time distribution of a randomly selected cell, $F_c(t)$ (the subscript c denotes the cell). Let T_c denote the failure-time of a randomly selected cell. Conditioning on a given $\boldsymbol{\theta}$ vector, the failure-time distribution at a mission time *t* for a randomly selected cell is given by

$$F_c(t|\boldsymbol{\theta}) = P_r(T_c \le t|\boldsymbol{\theta})$$
$$= \int P_r\left[h(t;\boldsymbol{\beta}) \le \eta_{f,2}\right] \times f(\beta|\boldsymbol{\theta}) d\boldsymbol{\beta} \quad (5.1)$$

Because $\boldsymbol{\theta}$ is a random vector whose posterior distribution is denoted by $f(\boldsymbol{\theta}|\boldsymbol{y})$ we can derive the posterior density for the cell failure-time distribution $F_c(t)$, i.e., $f(F_c(t)|\boldsymbol{y})$, via the transformation of random variables. Again, MCMC simulation algorithm was implemented to simulate a random sample from $f(F_c(t)|\boldsymbol{y})$ in order to perform the posterior inference on $F_c(t)$. According to the theory of order statistics, the failure-time distribution for a randomly selected stack is given by

$$F_{s,2}^c(t) = 1 - \sum_{j=0}^{k-1} \binom{m}{j} F_c t^j [1 - F_c(t)]^{m-j} \quad (5.2)$$

Here, the subscript '2' indicates that the failure-time distribution for the stack considers the minimum cell voltage measure only. The superscript 'c' implies that this distribution is obtained by using the "cell-level" approach instead of the "stack-level" approach in Equation (3.13).

Figure 7 compares the posterior medians of the stack failure-time distribution produced by the stack-level approach discussed in Section 3.4.1 and the cell-level approach discussed in this section with assuming k = 1, 2, 3. Interestingly, the two approaches produced almost identical prediction results for the stack failure-time distribution. It implies that the stack failure-time distribution considering only the minimum cell voltage measure can be analyzed under either the assumption of the continuous-state system or that of the binary-state system. However, the alternative cell-level approach has a limitation to predict the stack reliability based on the stack output voltage measure.

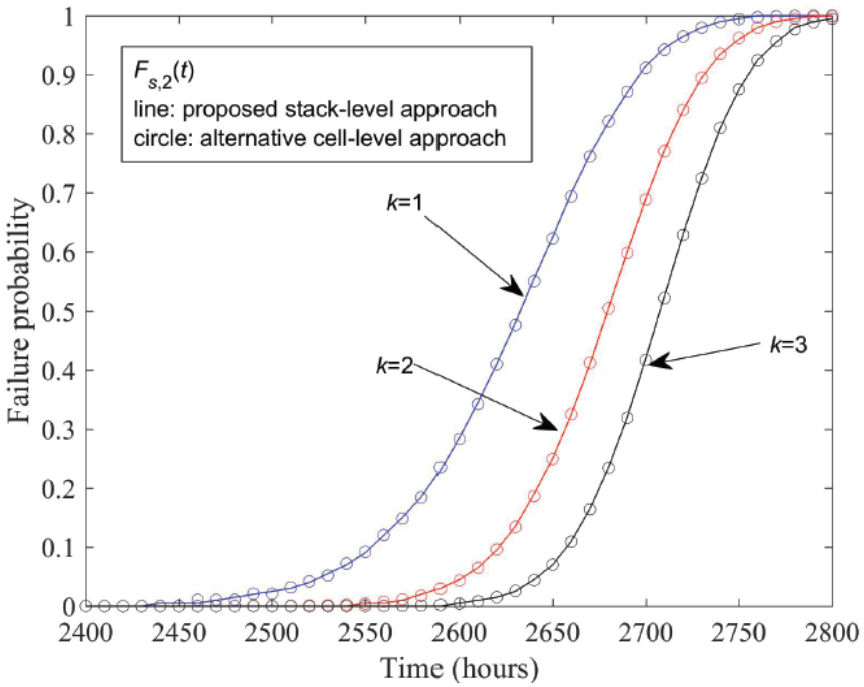

Figure 7. Posterior medians of the failure-time distributions for a randomly selected stack using two different approaches by considering the minimum cell voltage measure only

5.2 Failure-Time Prediction by Using the Stack Output

Another alternative method to predict the stack reliability through the stack output voltage measure is to sum the measured values of cell voltage at each inspection points to derive the stack output voltage degradation curve. Figure 8 presents the two-term exponential fit to the stack output voltage degradation data. Because only one stack was tested in this experiment, we have a limitation in predicting the failure-time distribution of a randomly selected stack by capturing the stack-to-stack variation. However, we are expected to use the two-term exponential to fit the stack output voltage degradation to predict the RUL of the tested stack, which will deserve future research.

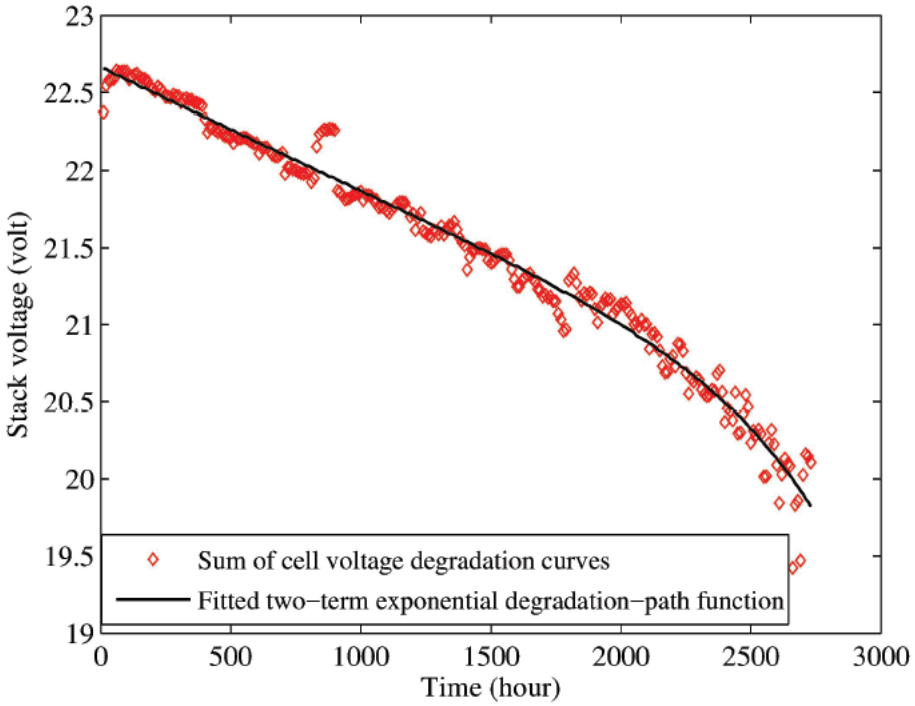

Figure 8. The stack output voltage degradation curve obtained by summing individual degradation levels of cell voltage and the fitted two-term exponential degradation-path function

5.3 Hierarchical Bayesian Analysis with Change-point General Degradation-Path model

The predicted stack failure-time distribution may be sensitive to the degradation model employed because the extrapolation from the fitting to degradation data is involved in its prediction. For the purpose of comparison, we employed another degradation model in the analysis, that is, the change-point general degradation-path model which is given by

$$h(t_{ij};\boldsymbol{\alpha}_i) = \begin{cases} \alpha_{i1} + \alpha_{i2}(t_{ij} - \gamma_i), & t_{ij} \le \gamma_{i,} \\ \alpha_{i1} + \alpha_{i3}(t_{ij} - \gamma_i), & t_{ij} > \gamma_{i,} \end{cases} \tag{5.3}$$

for $\boldsymbol{\alpha_i} \equiv (\alpha_{i1,}\alpha_{i2}, \alpha_{i3}, \gamma_i)$. The change-point model consists of two pieces of linear functions to describe the actual nonlinear degradation-path. Herein γ_i is the change-point separating the two linear pieces, α_{i1} is the actual degradation measure at the change-point

γ_i, α_{i2} and α_{i3} are the slopes before and after the change-point, respectively. The change-point model (5.3) explicitly expresses a continuity at the change-point. There have been the other forms of change-point models with or without the continuity constraints [73, 79, 80]. The change point models have been previously applied to model multi-phase degradation phenomena observed on some light displays such as vacuum fluorescent displays (VFDs), plasma display panels (PDPs), and organic light-emitting diodes (OLEDs) [5, 51, 81].

A three-stage hierarchical Bayesian degradation model was constructed, of which the first-stage model describes the cell voltage degradation using the change-point general degradation-path model (5.3). The second-stage model assumes that all the $\boldsymbol{\alpha_i}$ vectors in a stack form a random sample from the truncated multivariate normal distribution with a mean vector μ_α and a variance-covariance matrix Σ_α restricted to the region $\alpha \in \mathcal{A} \equiv \{\alpha_1 > 0, \alpha_2 < 0, \alpha_3 < 0, \gamma \in (0, \tau)\}$, where τ is the test duration. We assume that there is one change-point within the test duration $(0, \tau)$. Finally, the third-stage model assigns the inverse-gamma, multivariate normal, and scaled inverse-Wishart priors to σ^2, μ_α, and Σ_α respectively. Parameters of the prior distributions are selected according to Section 3.3 so that non-informative priors are employed. Failure-time distributions are estimated according to Section 3.4.1 with $h(t; \beta)$ replaced by the change-point regression (5.3).

The related mean squares from two degradation modeling are defined by

$$MS_i = \frac{1}{n_i}\sum_{j=1}^{n_i}(y_{ij} - \widetilde{h_i}(t_{ij}))^2, \tag{5.4}$$

where $\widetilde{h_i}(t)$ is the posterior medians of the actual degradation-path predicted by each model $i = 1, 2, \cdots, 32$.

Table E provides the mean squares from the two degradation modeling fits. The averaged mean squares over the 32 fuel cells are also reported at the last row of the Table E. For example, Figure 9 plots the posterior medians of the actual degradation-paths predicted by the two different degradation models for the fuel stack cell #1. Note that these two models provide very closets to the observed degradation data with almost identical averaged mean squares. However, the two models have substantial difference in extrapolation beyond the test duration, resulting in significant difference in reliability predictions. Figure 10 compares the posterior medians of $F_s(t)$ predicted using the two degradation models assuming $k = 1$ in k-out-of-m:F system. The two-term exponential degradation model yields lower reliability predictions than the change-point degradation model. In extrapolating beyond the test duration, the two-term exponential degradation model has a more rapid drop in voltage than the change-point degradation model, which is clearly shown in Figure 9.

Table E Mean squares of the two-term exponential model and the change-point regression model fitted to the cell degradation data

Cell	Two-term exponential model ($\times 10^{-4}$)	Change-point regression model ($\times 10^{-4}$)
1	6.691	6.690
2	8.031	8.038
3	9.097	9.094
4	8.219	8.220
5	10.42	10.41
6	9.663	9.663
7	7.426	7.426
8	11.14	11.13
9	9.371	9.374
10	4.105	4.101
11	10.85	10.85
12	10.51	10.51
13	12.83	12.83
14	11.07	11.08
15	6.855	6.855
16	8.977	8.977
17	6.011	6.011
18	7.648	7.651
19	6.430	6.424
20	12.90	12.90
21	6.395	6.405
22	7.269	7.273
23	6.207	6.228
24	9.565	9.561
25	8.338	8.337
26	7.201	7.199
27	10.82	10.82
28	5.571	5.575
29	5.556	5.558
30	3.861	3.866
31	0.475	0.472
32	0.153	0.150
Average	7.802	7.803

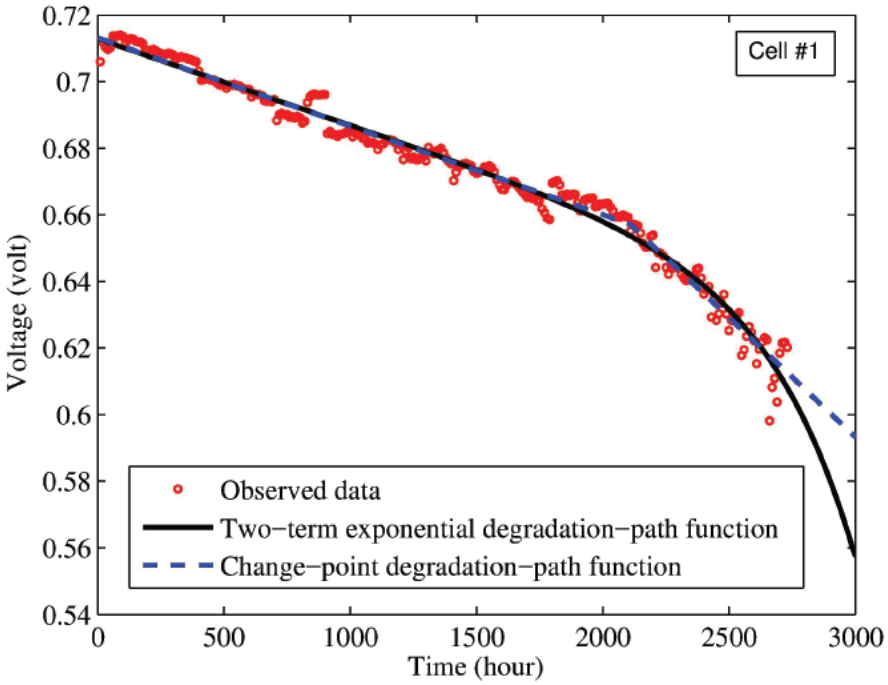

Figure 9. Comparison between the two degradation modeling fits_Posterior medians of two degradation models fitted to the degradation data of fuel stack cell #1

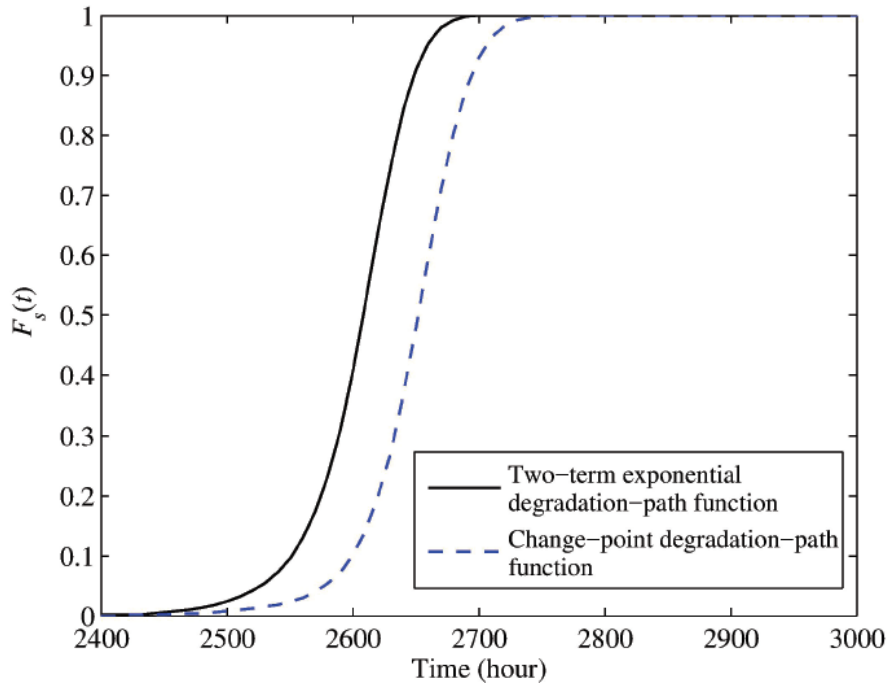

Figure 10. Comparison between the two degradation modeling fits_Posterior medians of the stack failure-time distribution $F_s(t)$ when $k = 1$

Based on our current knowledge and data, we might prefer the two-term exponential function due to the following two reasons. Firstly, the two-term exponential function has some close connections to the degradation mechanisms of different types of batteries and fuel cells. Secondly, the change-point regression analysis assumes an abrupt change of the actual degradation-path at the change point, which may not be reasonable in reality; while the two-term exponential function produces a smooth transition between the two phases.

CHAPTER 6: CONCLUSION

This dissertation developed a hierarchical Bayesian modeling and reliability data analysis method to predict the reliability of a PEMFC stack based on the voltage degradation data collected from its individual fuel stack cells. The fuel cell voltage degradation curve has the nonlinear pattern which is reasonably described by the two-term exponential model. The PEMFCs system has two degradation measures caused by the continuous degradation of the fuel stack cells. One is the stack output voltage which could not be measured directly from the system level, the other one is the minimum cell voltage and it is assessed at its component level. Soft failure is used to define the performance failure and the safety failure due to the continuous degradation model is used. Three possible alternative approaches were discussed with an in-depth comparison. This paper will contribute to the modeling and white-box reliability data analysis methods for continuous-state systems composed of continuous-state components.

In the current study, we assumed that the cells in a stack are independent and the stack-to-stack variation is completely caused by the cell-to-cell variation due to only one tested stack is monitored. When more experimental investigations are performed with more data available, we are expected to check those important assumptions. The failure-time distribution (3.11) derived from the Hierarchical Bayesian model and the failure-time distribution (3.15) based on the independence assumption of the two measures were compared to check if the independence exists between the two measure. The results showed that the two types of the failure-time distributions are very close but the independence could not be proved. Moreover, more physical failure analysis will be

performed to explore the degradation mechanisms so that we can fundamentally identify the exact degradation mechanisms of fuel cells.

In addition, Stochastic process is reviewed in Chapter 2 which is very popular on degradation analysis. Compared with the general degradation-path model which uses the mean regression function to fit the degradation data, the difference is that noise is included in the Stochastic process model and the corresponding degradation model may hit the threshold more than one time. The challenge by using the stochastic process is how to fit the nonlinear degradation pattern adequately. Thus, apply Stochastic process to model the degradation-path of the fuel stack is expected to be considered as one of the future research directions.

Besides that, the methodology proposed in this research is based on a real degradation test. Thus, it could be extended to use for future study about optimal system design or system maintenance.

REFERENCES

[1] W. Kuo and M. J. Zuo, *Optimal Reliability Modeling*, Wiley, Hoboken, 2003.

[2] M. Rausand and A. Hoyland, *System Reliability Theory*, Wiley, Hoboken, 2003.

[3] S.J. Bae, S.-J. Kim, J.-H. Lee, I. Song, N.-I. Kim, Y. Seo, K.B. Kim, N. Lee, and J.-Y. Park, "*Degradation Pattern Prediction of a Polymer Electrolyte Membrane Fuel Cell Stack with Series Reliability Structure via Durability Data of Single Cells*," Applied Energy, vol. 131, pp. 48-55, Oct. 2014.

[4] W. Kuo, W. T. K. Chien, and T. Kim, *Reliability, Yield, and Stress Burn-in*, Kluwer Academic Publishers, Boston, 1998.

[5] S. J. Bae and P. H. Kvam, "*A Change-Point Analysis for Modeling Incomplete Burn-in for Light Displays*," IIE Transactions, vol. 38, no. 6, pp. 489-498, 2006.

[6] M. J. Zuo, R. Jiang, and R. C. M. Yam, "*Approaches for Reliability Modeling of Continuous-State Devices*," IEEE Transactions on Reliability, vol. 48, no. 1, pp. 9-18, Mar. 1999.

[7] A., J. B. Carlin, H. S. Stern, and D. B. Rubin, *Bayesian Data Analysis*, Chapman & Hall Texts in Statistical Science Series, Second Edition, London, New York, 1995.

[8] E. Zio, M. Marella, and L. Podofillini, "*A Monte Carlo Simulation Approach to the Availability Assessment of Multi-State Systems with Operational Dependencies*," Reliability Engineering and System Safety, vol. 92, pp. 871-882, 2007.

[9] M. E. Irwin, "*Prior Choice, Summarizing the Posterior*," Spring 2005.

[10] M. S. Nikulin, N. Limnios, N. Balakrishnan, K. Waltraud, and C. Huber-Carol, *Advances in Degradation Modeling*, SpringerLink, Boston: Birkhäuser, 2010.

[11] M.A. Freitas, M.L. de Toledo, E.A. Colosimo, and M.C Pires, "*Using Degradation Data to Assess Reliability: A Case Study on Train Wheel Degradation*," Quality and Reliability Engineering International, vol. 25, no. 5, pp. 607-629, Dec. 2009.

[12] H.F. Yu, "*Designing an Accelerated Degradation Experiment with a Reciprocal Weibull Degradation Rate*," Journal of Statistical Planning and Inference, vol. 136, no. 1, pp. 282-297, Jan. 2006.

[13] C. Lu and W. Meeker, "*Using Degradation Measures to Estimate a Time-to-Failure Distribution*," Technometrics, vol. 35, no. 2, pp. 161-174, 1993.

[14] M. A. Ebrahem, M. T. Alodat, and A. Arman, "*Estimating the Time-to-Failure Distribution of a Linear Degradation Model Using a Bayesian Approach*," Applied Mathematical Sciences, vol. 3, no. 1, pp. 27-42, Jan. 2009.

[15] F. Haghighi and M. Nikulin, "*On the Linear Degradation Model with Multiple Failure Modes*," Journal of Applied Statistics, vol. 37 no. 9, pp. 1499-1507, Sep. 2010.

[16] V. Bagdonaviciusa, A. Bikelisa, V. Kazakeviciusa, and Mikhail Nikulin, "*Analysis of Joint Multiple Failure Mode and Linear Degradation Data with Renewals*," Journal of Statistical Planning and Inference, vol. 137, no. 7, pp. 2191-2207, Jul. 2007.

[17] C. Peng and S. Tseng, "*Mis-Specification Analysis of Linear Degradation Models*," IEEE Transactions on Reliability, vol. 58, no. 3, pp. 444-455, Sep. 2009.

[18] L. B. Dakhn, M. A. Ebrahem, and O. Eidous, "*Semi-Parametric Method to Estimate the Time-to-Failure Distribution and Its Percentiles for Simple Linear Degradation Model*," Journal of Modern Applied Statistical Methods, vol. 16, no. 2, pp. 322–346, Nov. 2017.

[19] X. Si, W. Wang, C. Hu, and D. Zhou, "*Remaining Useful Life Estimation Based on a Nonlinear Diffusion Degradation Process*," IEEE Transactions on Reliability, vol. 61, no. 1, pp. 50-67, Mar. 2012.

[20] S. J. Bae, S. Kim, M. Kim, B. Lee, and C. W. Kang, "*Degradation Analysis of Nano-Contamination in Plasma Display Panels*", IEEE Transactions on Reliability, vol. 57, no. 2, pp. 222-229, Jun. 2008.

[21] S. J. Bae, T. Yuan, S. Ning, and W. Kuo, "*A Bayesian Hierarchical Approach to Modeling Two-Phase Degradation Using Change-Point Regression*", Reliability Engineering and System Safety, vol. 134, pp. 66-74, Feb. 2015.

[22] S. J. Bae, S. J. Kim, S. K. Um, J. Y. Park, J. H. Lee, and H. Cho, "*A Prediction Model of Degradation Rate for Membrane Electrode Assemblies in Direct Methanol Fuel Cells*," International Journal of Hydrogen Energy, vol. 34, no. 14, pp. 5749-5758, Jul. 2009.

[23] W. He, N. Williard, M. Osterman, and M. Pecht, "*Prognostics of Lithium-ion Batteries based on Dempster-Shafer Theory and the Bayesian Monte Carlo Method*," Journal of Power Sources, vol. 196, no. 23, pp. 10314-10321, Dec. 2011.

[24] S.J. Bae and P.H. Kvam, "*A Nonlinear Random-Coefficients Model for Degradation Testing*," Technometrics, vol. 46, no. 4, pp. 460-469, Nov. 2004.

[25] Z. Xu, Y. Hong, and R. Jin, "*Nonlinear General Path Models for Degradation Data with Dynamic Covariates*," Applied Stochastic Models in Business and Industry, vol. 32, no. 2, Aug. 2015.

[26] G.A. Pavliotis, *Stochastic Processes and Applications: Diffusion Processes, the Fokker-Planck and Langevin Equations*, Berlin, Springer, 2014.

[27] L. Liu, X. Li, F. Sun, and N. Wang, "*A General Accelerated Degradation Model Based on the Wiener Process*," Materials, vol. 9, no. 12, pp. 981-1001, 2016.

[28] H. U. Gerber, M. Goovaerts, and N. DePril, "*Degradation Data Analysis Using Wiener Processes With Measurement Errors*," IEEE Transactions on Reliability, vol. 62, no. 4, pp.772-780, Dec. 2013.

[29] S. Tang, X. Guo, and Z. Zhou, "*Mis-Specification Analysis of Linear Wiener Process-Based Degradation Models for the Remaining Useful Life Estimation*," Risk and Reliability, vol. 228, no. 5, pp. 478-487, Oct. 2014.

[30] K. L. Son, M. Fouladirad, A. Barros, E. Levrat, and B. Iung, "*Remaining Useful Life Estimation Based on Stochastic Deterioration Models: A Comparative Study*," Reliability Engineering and System Safety, Vol. 112, pp. 165-175, Apr. 2013.

[31] G. A. Whitmore and F. Schenkelberg, "*Modeling Accelerated Degradation Data Using Wiener Diffusion with A Time Scale Transformation*," Kluwer Academic Publishers, vol. 3, pp. 27-45, 1997.

[32] N. Z. Gebraeel, M. A. Lawley, L. Rong, and K. Jennifer, "*Residual-Life Distributions from Component Degradation Signals: A Bayesian Approach*," IIE Transactions, vol. 37, no. 6, pp. 543-557, 2005.

[33] K. A. Doksum and A. Hbyland, "*Models for Variable-Stress Accelerated Life Testing Experiments Based on Wiener Processes and The Inverse Gaussian Distribution*," Technometrics, vol. 34, no. 1, pp. 74-82, Feb. 1992.

[34] G. Whitmore and F. Schenkelberg, "*Modelling Accelerated Degradation Data Using Wiener Diffusion with A Time Scale Transformation*," Lifetime data analysis, vol. 3, no. 1, pp. 27-45, Jan. 1997.

[35] X. S. Si, W. Wang, C. H. Hu, D. H. Zhou, and M. G. Pecht, "*Remaining Useful Life Estimation Based on A Nonlinear Diffusion Degradation Process*," IEEE Transactions on Reliability, vol. 61, no. 1, pp. 50–67, Mar. 2012.

[36] X. Wang, N. Balakrishnan, and B. Guo, "*Residual Life Estimation based on a Generalized Wiener Degradation Process*," Reliability Engineering and System Safety, vol. 124, pp. 13-23, Apr. 2014.

[37] S. Tang, X. Guo, C. Yu, Z. Zhou, and B. Zhang, "*Real Time Remaining Useful Life Prediction Based on Nonlinear Wiener Based Degradation Processes with Measurement Errors*," Journal of Central South University, vol. 21, no. 12, pp. 4509-4517, Dec. 2014.

[38] S. Tang, X. Guo, C. Yu, H. Xue, and Z. Zhou, "*Accelerated Degradation Tests Modeling Based on The Nonlinear Wiener Process with Random Effects*," Mathematical Problems in Engineering, vol 2014, no. 560726, May 2014.

[39] Z. Zhang, Xiao. Si, and C. Hu, "*An Age- and State-Dependent Nonlinear Prognostic Model for Degrading Systems*," IEEE Transactions on Reliability, vol. 64, no. 4, pp. 1214-1228, Dec. 2015.

[40] W. Peng, Y. Li, Y. Yang, H. Huang, and M. Zuo, "*Inverse Gaussian Process Models for Degradation Analysis: A Bayesian Perspective*," Reliability Engineering and System Safety, vol. 130, pp. 175-189, Oct. 2014.

[41] D. Pan, J. Liu, and J. Cao, "*Remaining Useful Life Estimation Using and Inverse Gaussian Degradation Model*," Neurocomputing, vol. 185, pp.64-72, Apr. 2016.

[42] X. Wang and D. Xu, "*An Inverse Gaussian Process Model for Degradation Data*", Technometrics, vol. 52, no. 2, pp. 188-197, May 2010.

[43] W. Peng, Y. Li, Y. Yang, J. Mi, and H. Huang, "*Bayesian Degradation Analysis with Inverse Gaussian Process Models Under Time-Varying Degradation Rates*", IEEE Transactions on Reliability, vol. 66, no. 1, pp. 84-96, Mar. 2017.

[44] D. Pan, J. Liu, and J. Cao, "*Remaining Useful Life Estimation Using an Inverse Gaussian Degradation Model*," Neurocomputing, vol. 185, pp.64-72, Apr. 2016.

[45] C. Park and W.J. Padgett, "*Accelerated Degradation Models for Failure Based on Geometric Brownian Motion and Gamma Processes*," Lifetime Data Analysis, vol. 11, no. 4, pp. 511-527 Dec. 2005.

[46] J. F. Lawless and M. J. Crowder, "*Covariates and Random Effects in A Gamma Process Model with Application to Degradation and Failure*," Lifetime Data Analysis, vol. 10, no. 3, pp. 213-227, Sep. 2004.

[47] Z. Pan and N. Balakrishnan, "*Reliability Modeling of Degradation of Products with Multiple Performance Characteristics Based on Gamma Processes*," Reliability Engineering and System Safety, vol. 96, no. 8, pp. 949-957, Aug. 2011.

[48] J.M. Noortwijka, J.A.M. Weideb, M.J. Kallena, and M.D. Pandey, "*Gamma Processes and Peaks-over-Threshold Distributions for Time-Dependent Reliability*", Reliability Engineering and System Safety vol. 92, pp. 1651–1658, 2007.

[49] H. Wang, T. Xu, and Q. Mi, "*Lifetime Prediction Based on Gamma Processes from Accelerated Degradation Data*", Chinese Journal of Aeronautics, vol. 28, no. 1, pp.172–179, 2015.

[50] B. Sun, M. Yan, Q. Feng, Y. Li, Y. Ren, K. Zhou, and W. Zhang, "*Gamma Degradation Process and Accelerated Model Combined Reliability Analysis Method for Rubber O-Rings*," IEEE Access, vol. 6, pp. 10581-10590, Jan. 2018.

[51] M. Mahmoodian and A. Alani, "*Modeling Deterioration in Concrete Pipes as A Stochastic Gamma Process for Time-Dependent Reliability Analysis*", Journal of Pipeline Systems Engineering and Practice, vol. 5, no. 1, pp. 1-5, Feb. 2014.

[52] S.J. Bae, T. Yuan, S. Ning, and W. Kuo, "*A Bayesian Approach to Modeling Two-Term Degradation Using Two-Term Exponential*," Reliability Engineering and System Safety, vol. 124, pp. 66-74, Feb. 2015.

[53] T. Yuan and Y. Ji, "*A Hierarchical Bayesian Degradation Model for Heterogeneous Data*," IEEE Transactions on Reliability, vol. 64, no. 1, pp. 63-70, Mar. 2015.

[54] M. T. Lee, M. Shubina1, and A. Zaslavsky, "*Bayesian Analysis for Markers and Degradation*," Markers and Degradation, pp. 1262-1271, 2000.

[55] Y. Shi and W.Q. Meeker, "*Bayesian Methods for Accelerated Destructive Degradation Test Planning*," IEEE Transactions on Reliability, vol. 61, no. 1, pp. 245-253, Mar. 2012.

[56] C. J. Lu, W. Q. Meeker, and L. A. Escobar, "*A Comparison of Degradation and Failure-Time Analysis Methods for Estimating A Time-to-Failure Distribution*," Statistica Sinica, vol. 6, no. 3, pp. 531-546, Jul. 1996.

[57] Y. Wang and H. Pham, *"Modeling the Dependent Competing Risks with Multiple Degradation Processes and Random Shock Using Time-Varying Copulas*," IEEE Transactions on Reliability, vol. 61, no. 1, pp. 13-22, 2012.

[58] H. Liao, E. A. Elsayed, and C. Ling-Yau, "*Maintenance of Continuously Monitored Degrading Systems*," European Journal of Operational Research, vol. 174, no. 2, pp. 821-836, Oct. 2006.

[59] P. Wang and D. W. Coit, "*Reliability Prediction based on Degradation Modeling for Systems with Multiple Degradation Measures*," Proceedings of Annual Reliability and Maintainability Symposium, pp. 302-307, Jan. 2004.

[60] H. Gao, L. Cui, and Q. Qiu, "*Reliability Modeling for Degradation-Shock Dependence Systems with Multiple Species of Shocks*," Reliability Engineering and System Safety, vol. 185, pp. 133-143, May 2019.

[61] X. Zhao, S. He, and M. Xie, "*Utilizing Experimental Degradation Data for Warranty Cost Optimization under Imperfect Repair*," Reliability Engineering and System Safety, vol. 177, pp. 108-119, Sep. 2018.

[62] H. Peng, D. W. Coit, and Q. Feng, "*Component Reliability Criticality or Importance Measures for Systems with Degrading Components*," IEEE Transactions on Reliability, vol. 61, no. 1, pp. 4-12, Mar. 2012.

[63] X. Zhao, B. Liu, and Y. Liu, "*Reliability Modeling and Analysis of Load-Sharing Systems with Continuously Degrading Components*," IEEE Transactions on Reliability, vol. 67, no. 3, pp. 1096-1110, Sep. 2018.

[64] Q. Sun, Z.-S. Ye, and N. Chen, "*Optimal Inspection and Replacement Policies for Multiunit Systems Subject to Degradation*," IEEE Transactions on Reliability, vol. 67, no. 1, pp. 401-413, 2018.

[65] E. Nezakati, M. Razmkhah, and F. Haghighi, "*Reliability Analysis of A k-out-of-n:F System Under A Linear Degradation Model with Calibrations*," IEEE Transactions on Reliability, vol. 55, no. 2, pp.314-318, Jul. 2006.

[66] K. Yang and J. Xue, "*Continuous-state Reliability Analysis*," Proceedings of Annual Reliability and Maintainability Symposium, pp. 251-257, Jan. 1996.

[67] R. D. Brunelle and K. C. Kapur, "*Continuous-State System-Reliability: An Interpolation Approach," IEEE Transactions on Reliability*, vol. 47, no. 2, pp. 181-187, Jun. 1998.

[68] M. L. Gámiz and M. D. Martínez Miranda, "*Regression Analysis of the Structure Function for Reliability Evaluation of Continuous-State System*," Reliability Engineering and System Safety, vol. 95, no. 2, pp. 134-142, 2010.

[69] C. Han and H. Lee, "*A Field-Applicable Health Monitoring Method for Photovoltaic System*," Reliability Engineering and System Safety, vol. 184, pp. 219-227, 2019.

[70] B. Sun, X. Fan, H. Ye, J. Fan, C. Qian, W. van Driel, and G. Zhang, "*A Novel Lifetime Prediction for Integrated Led Lamps by Electronic-Thermal Simulation*," Reliability Engineering and System Safety, vol. 163, pp. 14-21, Jul. 2017.

[71] M. Guida, F. Postiglione, and G. Pulcini, "*A Random-Effects Model for Long-Term Degradation Analysis of Solid Oxide Fuel Cells*," Reliability Engineering and System Safety, vol. 140, pp. 88-98, Aug. 2015.

[72] M. Jouin, R. Gouriveau, D. Hissel, M. Pera, and N. Zerhouni, "*Degradation Analysis and Aging Modeling for Health Assessment and Prognostics of PEMFC*," Reliability Engineering and System Safety, vol. 148, pp. 78-95, 2016.

[73] B. P. Carlin, A. E. Gelfand, and A. F. M. Smith, "*Hierarchical Bayesian Analysis of Changepoint Problems*," Journal of the Royal Statistical Society: Applied Statistics, vol. 41, no. 2, pp. 389-405, 1992.

[74] Multivariate normal distribution: https://en.wikipedia.org/wiki/Multivariate_normal_distribution#Bayesian_inference.

[75] N. Z. Gebraeel and M. A. Lawley, "*Residual-Life Distribution from Component Degradation Signals: A Bayesian Approach*," IIE Transactions, vol. 37, no. 6, pp. 543-557, Jun. 2005.

[76] D. Spiegelhalter, A. Thomas, N. Best, and D. Lunn, *WinBUGS User Manual*, internet: http://www.mrc-bsu.cam.ac.uk/bugs, version 1.4, Jan. 2003.

[77] D. Lunn, D. Spiegelhalter, A. Thomas, and N. Best, "*The BUGS Project: Evolution, Critique and Future Directions*," Statistics in Medicine, vol. 28, no. 25, pp. 3049-3067, 2009.

[78] J. C. Pinheiro and D. M. Bates, "*Approximations to the Log-Likelihood Function in the Nonlinear Mixed-Effects Model*," Journal of Computational & Graphical Statistics, vol. 4, no.1, pp.12-35, Mar 1995.

[79] A. Beem, "*A Program for Fitting Two-term Segmented-Curve Models with An Unknown Change Point, with An Application to the Analysis of Strategy Shift in A*

Cognitive Task," Behavior Research Methods, Instruments, and Computers, vol. 27, no. 3, pp. 392-399, Sep. 1995.

[80] V. M. R. Muggeo, "*Estimating Regression Models with Unknown Break-Points*," Statistics in Medicine, vol. 22, no. 19, pp. 3055-3071, Oct. 2003.

[81] S. J. Bae, T. Yuan, and S. J. Kim, "*Bayesian Degradation Modeling for Reliability Prediction of Organic Light-Emitting Diodes*," Journal of Computational Science, vol. 17, pp. 117-125, 2016.

APPENDIX

1. Sample $\boldsymbol{\vartheta}_i = (\alpha_i, \beta_{1i}, \beta_{2i})'$ from the conditional posterior distribution $f(\boldsymbol{\vartheta}_i|\sigma^2, \gamma_i, \boldsymbol{\mu}, \boldsymbol{\Sigma}, \mathbf{d})$, *i*=1, 2, …, *m*.

2. Sample γ_i from the conditional posterior distribution $f(\gamma_i|\sigma^2, \boldsymbol{\upsilon}_i, \boldsymbol{\mu}, \boldsymbol{\Sigma}, \mathbf{d})$, *i*=1, 2, …, *m*.

3. Sample σ^2 from the conditional posterior distribution

$$(\sigma^2|\theta_1, \ldots, \theta_m, \mathbf{d}) \sim Ig\left(a_\sigma + \sum_{i=1}^{m} \frac{n_i}{2}, b_\sigma + \sum_{i=1}^{m} \frac{(y_i - X_i(\gamma_i)\vartheta_i)'(y_i - X_i(\gamma_i)\vartheta_i}{2}\right).$$

4. Sample $\boldsymbol{\mu}$ from the conditional posterior distribution

$$(\boldsymbol{\mu}|\theta_1, \ldots, \theta_m, \boldsymbol{\Sigma}, \mathbf{d}) \propto [P(\mu, \sum)]^{-m} \, exp\left[-\frac{\sum_{i=1}^{m}(\theta_i - \mu)\sum^{-1}(\theta_i - \mu) + (\mu - \mu_\mu)\sum_\mu{}^{-1}(\mu - \mu_\mu)}{2}\right].$$

5. Sample $\mathbf{Q}$ from the conditional posterior distribution:

$$f(\mathbf{Q}|\boldsymbol{\theta}_1^*, \ldots, \boldsymbol{\theta}_m^*, \boldsymbol{\mu}, \delta_1, \ldots, \delta_\vartheta, \mathbf{d}) \sim IW(\rho + m, S + \Delta^{-1}(\sum_{i=1}^{m}(\theta_i^* - \mu)(\theta_i^* - \mu)')\Delta^{-1}).$$

6. Sample δ_i from the conditional posterior distribution:

$$f(\delta_i|\boldsymbol{\theta}_1^*, \ldots, \boldsymbol{\theta}_m^*, \boldsymbol{\mu}, \{\delta_j; j \neq i\}, \mathbf{d}) \propto \delta_i^{-m+a_\delta-1} \, exp\left[-\left(b_\delta\delta_i + \frac{\Lambda_{ij}[Q^{-1}]_{ii}}{2\delta_i^2} + \frac{1}{\delta_i}\sum_{i\neq j}[Q^{-1}]_{ij}\Lambda_{ij}/\delta_j\right)\right].$$

Thesis and Dissertation Services